ELECTROMOTIVE FORCE MEASUREMENTS OF METAL-OXYGEN SYSTEMS

DISSERTATION

Presented in Partial Fulfillment of the Requirements for the Degree Doctor of Philosophy in the Graduate School of The Ohio State University

By

Kazuhiro Goto, B. Eng., M. Eng.

****

The Ohio State University
1962

Approved by

George R. St. Pierre
Adviser
Department of Metallurgical Engineering

Dedicated to

Harumi

ACKNOWLEDGMENT

The author acknowledges with sincere appreciation the invaluable contribution of Professor George R. St. Pierre.

Acknowledgment is made to Mr. John D. Birle of the Engineering Experimental Station for chemical analyses of lead-tin alloys and stabilized zirconia.

CONTENTS

TABLES

ILLUSTRATIONS

ILLUSTRATIONS (contd.)

CHAPTER I

INTRODUCTION, PRINCIPLE OF EXPERIMENTS, AND PRELIMINARY EXPERIMENTS

Introduction

Metals are commonly associated with oxygen in ores. Although the naturally occurring minerals are often very complex, the chemistry of metallic oxides is of great importance in the study of process metallurgy. Throughout most metallurgical processes the reduction of metallic oxides and the control of oxygen partial pressure are of paramount consideration. When complex oxides systems are subjected to a low oxygen partial pressure at elevated temperature, two immiscible liquid phases generally are formed. One phase, often designated as the slag, consists of a solution of highly stable metal oxides, while the other is a metallic solution formed from the metals with less stable oxides. From this simple description of a broad class of metallurgical processes, it is clear that a thorough knowledge of the chemical stabilities of metallic oxides and the chemical potentials of components within metallic solutions is essential to metallurgists. This is especially clear when one recognizes that the metallurgist must selectively extract one or more metals from the complex starting system. Although there are many other variables and design factors, temperature, oxygen partial pressure, and chemical potentials of metallic components are major control factors.

Therefore, a number of investigations have been devoted to the study of the thermodynamics and kinetics of oxidation-reduction reactions of metal-oxygen systems. The standard free energies of formation of many metal oxides have been determined by numerous investigators. The standard free energy indicates the relative stability of the oxides under certain restraints.

Recently, Elliott and Gleiser[1] have published an excellent compilation of thermodynamic data which includes the properties of many metal oxides. The chemical potentials of components in metallic solutions have been studied extensively also and the reader is directed toward the compilation of Kubaschewski[2] for a thorough treatment.

The intention of this dissertation is to present an experimental approach which is of considerable value in studying metal-oxygen systems. In particular, it is shown that electromotive force measurements on suitably constructed oxygen concentration cells can be used to determine (1) the standard free energy of formation of metal oxides; (2) the chemical potentials of components within liquid metallic solutions; and (3) the oxygen partial pressure in complex gas mixtures including CO, CO_2, H_2, and H_2O. Other authors[5,6,7] have demonstrated the suitability of this technique in other systems and situations. In particular, the present work will present data obtained for several metal oxides, for the activity of tin in liquid tin-lead alloys, and for an original oxygen gauge design.

Experimental Principle

An oxygen concentration cell consists of two electrodes separated by an electrolyte through which the transference of electrical charge is accomplished predominantly by the migration of oxygen ions.

Schematically, the cell can be shown as follows:

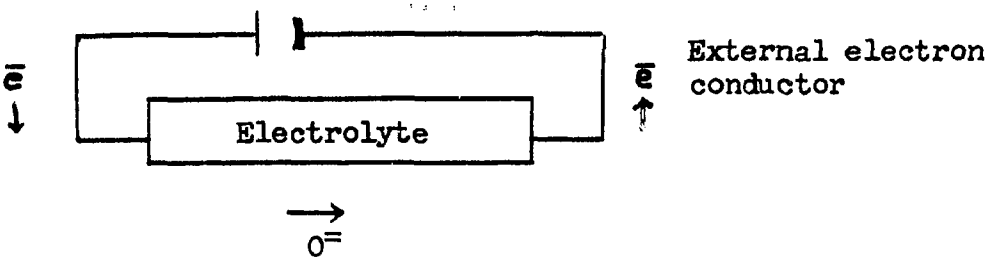

The electron flowing through the circuit is matched by $O^{=}$ migration.

It has been known [5,6,7,20,21] that the ZrO_2 - CaO solid electrolyte provides pure oxygen anion conduction due to oxygen vacancies at high temperatures. Thus, the study of the oxygen concentration cell with this electrolyte may have great significance in metallurgical research at high temperature (above 600°C).

As examples of the application of this anion conductor to the research, the following several types of measurement are conceivable.

1. Measurement of the standard free energy of formation of various metal oxides at elevated temperature from the standard free energy of the reaction between the metal and the oxide of a different metal. This method was used by Kiukkola and Wagner[6] using the following type of the cell.

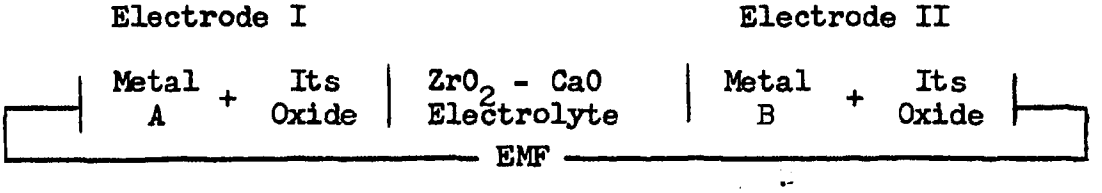

In the case that all substances are in solid state and the chemical equilibrium is attained at both electrodes, the EMF is simply determined by the equation

$$\Delta F^{\circ} = -NE\mathcal{F} \qquad (1)$$

where ΔF° is the difference between the standard free energy of formation of both the metal oxides.

$$\text{At Electrode I} \quad M_A + 0 = M_A0 \qquad \Delta F^{\circ}_A \qquad (2)$$

$$\text{At Electrode II} \quad M_B + 0 = M_B0 \qquad \Delta F^{\circ}_B \qquad (3)$$

$$M_A + M_B0 = M_B + M_A0 \quad \Delta F^{\circ} \qquad (4)$$

In the present work, these standard free energies were measured in the temperature range of 700° to 1200°C for the reactions

$$Cu_20 + Ni = 2Cu + NiO \qquad (5)$$

$$NiO + Fe = FeO + Ni \qquad (6)$$

$$PbO + 1/2\ Sn = Pb + 1/2SnO_2 \qquad (7)$$

From ΔF°, ΔF°_A can be obtained, if ΔF°_B is known and visa versa, with more accuracy than with some of the conventional methods.

2. Activity measurement of alloy or slag systems at solid or liquid state.

To measure the activity of a metal in solid or liquid alloy system, the following Galvanic cell is conceivable.

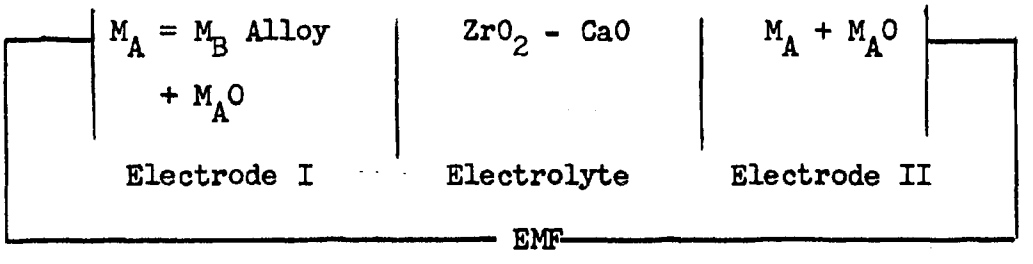

An expression for the EMF can be obtained from the consideration of the equilibrium existing within each electrode.

$$M_A + O = M_AO \tag{8}$$

$$K = \frac{a_{MAO}}{a_{MA}a_O} \tag{9}$$

The activity of oxygen on the right side of the cell equals

$$a_{O_{right}} = \frac{a_{MAO}}{Ka_{MA}} = \frac{1}{K} \tag{10}$$

if M_A and M_AO exist in pure state with unit activity.

Furthermore,

$$a_{O_{left}} = \frac{aM_AO}{Ka_{M_A}\,(alloy)} = \frac{1}{Ka_{M_A}\,(alloy)} \tag{11}$$

The actual cell reaction may be expressed as an oxygen concentration cell.

$$O_{left}\ (\text{in alloy} + M_AO) \longrightarrow O_{right}\ (\text{in } M_A + M_AO) \tag{12}$$

$$\Delta F = NE_O\mathcal{F} - NE\mathcal{F} = RT \ln \frac{a_{O(right)}}{a_{O(left)}} \tag{13}$$

$$E = \frac{-RT}{N\mathcal{F}} \ln a_{M_A}\,(alloy) \tag{14}$$

The same discussion is valid in measuring the activity of the slag system. In the present work, the molten lead-tin system has been studied.

3. Direct measurement of actual oxygen potential in high temperature atmosphere.

Since the method used in the present work is the oxygen concentration cell and EMF is very sensitive to the experimental atmosphere,

it may be possible to measure the oxygen potential in a high temperature gas with the appropriate technique.

In the present work, the following oxygen concentration cells have been constructed to measure the oxygen pressure in high temperature gases, and calibration curves of EMF against gas composition have been obtained with good reproducibility.

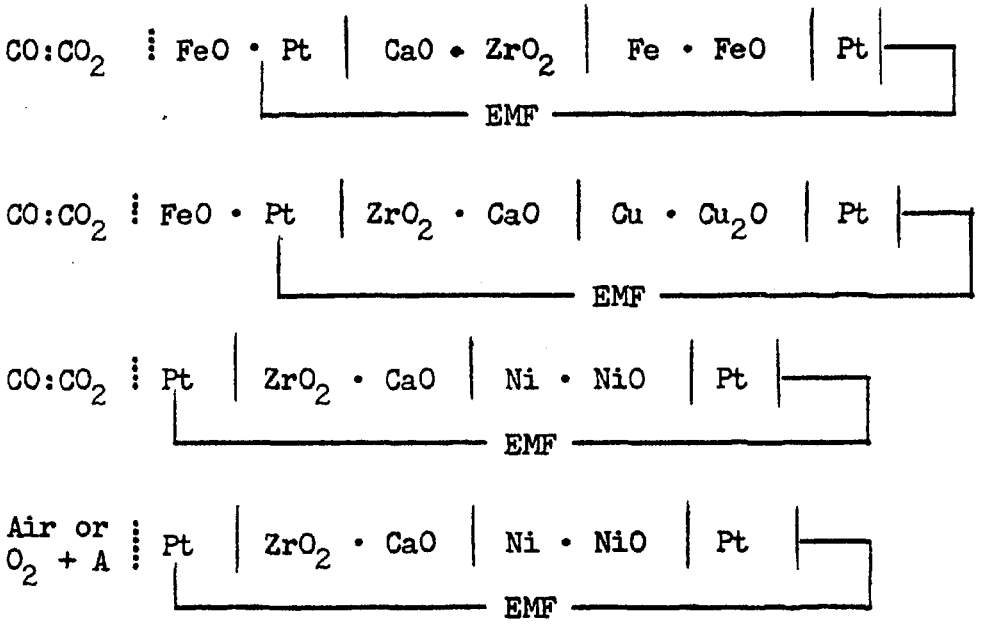

The partial pressure of oxygen in the right-hand side electrodes is determined by the equilibrium oxygen pressure of the metal oxide and metal, and the EMF may be directly determined by the oxygen pressure in the gas on the left-hand side electrode. The details will be shown in Chapter III.

Preliminary Experiments

The objectives of the preliminary experiment are (1) to determine the performance of the commercial stabilized zirconia as a pure anion conductor; (2) to check whether the gas cleaning train works satisfactorily; and (3) to determine the general characteristics of the

oxygen concentration cell technique. The EMF as a function of temperature has been studied for the following cells.

$$\text{Pt} \mid \text{Fe} \cdot \text{FeO} \mid \text{ZrO}_2 - \text{CaO} \mid \text{Ni} \cdot \text{NiO} \mid \text{Pt} \mid$$

$$\text{Pt} \mid \text{Ni} \cdot \text{NiO} \mid \text{ZrO}_2 - \text{CaO} \mid \text{Cu} \cdot \text{Cu}_2\text{O} \mid \text{Pt} \mid$$

$$\text{Pt} \mid \text{Pb} \cdot \text{PbO} \mid \text{ZrO}_2 - \text{CaO} \mid \text{Sn} \cdot \text{SnO}_2 \mid \text{Pt} \mid$$

Experimental apparatus. The schematic diagram of the experiment is shown in Figure 1 and Photograph 1. The apparatus consists of (1) gas cleaning and controlling trains, (2) Globar furnace, (3) electric power source, and (4) EMF measuring circuit.

The gas trains have three independent trains, i.e., for carbon monoxide, carbon dioxide, and argon. For the preliminary experiments, only the train for argon was used.

Commercial argon was cleaned through (1) iron and titanium chips held at 700 to 800°C, (2) concentrated H_2SO_4, and (3) $CaCl_2$ and anhydron. The flow rate was regulated by a capillary flow meter and bubbling bleeder.

Figures 2 and 3 show the diagram of the furnace, reaction chamber, and oxygen concentration cells. The reaction chamber is a pure alumina cylinder with water-cooled brass end caps. The dimensions of the cylinder are 1.8 inches outside diameter and 36 inches long.

The cell was supported by the lower porcelain tube, and argon gas was injected by a quartz tube in order to prevent mixing of the atmosphere between the two electrodes.

The complete cleaning of argon and the method of the argon injection are very important in obtaining a stable and consistent EMF.

The temperature was measured by a Pt-Pt 10% Rh thermocouple which was positioned just below the cell, and the temperature of the furnace was controlled by an outside thermocouple connected to an automatic regulator. The fluctuation of the measured temperature was less than $\pm$ 1°C at 700° to 1200°C. The EMF of the cell was measured by a potentiometer with an external Galvanometer, a standard cell, and a storage battery. The EMF could be measured to $\pm$ 0.00001 volt.

The inside pressure of the reaction chamber was always maintained about 3.0 cm Hg higher than the atmospheric pressure to prevent the back diffusion of the outside air.

Preparation of the cells and experimental procedure. A diagram of the cells is shown in Figure 3. The ZrO_2 - CaO electrolyte tablet was prepared from the stabilized zirconia powder of minus one hundred mesh. The composition of the stabilized zirconia is 93.68% $\pm$ 0.7% ZrO_2, 5.00% $\pm$ 0.01% CaO, $TiO_2 < 1.0\%$, and 0.07% ignition loss. All metal powders and oxide powders used were chemically pure and of -100 mesh. Discs of Ni - NiO were prepared by thoroughly mixing 2.000 gm of each and compacting in a die one inch in diameter. Discs of Cu - Cu_2O were similarly prepared. The discs were then pressed together at a pressure of 14.000 psi to form the cell NiO · Ni | ZrO_2 · CaO | Cu · Cu_2O with a rectangular platinum sheet and lead wire on both ends of the compact. As a binder, a small amount of water or alcohol was sometimes used.

For the | FeO · Fe | ZrO_2 - CaO | Ni · NiO | cell, the mixture of Fe and FeO was stamped into the pure alumina crucible and covered by the zirconia powder. The mixture of Ni and NiO was stamped into the stabilized zirconia crucible, the outside diameter of which is smaller than

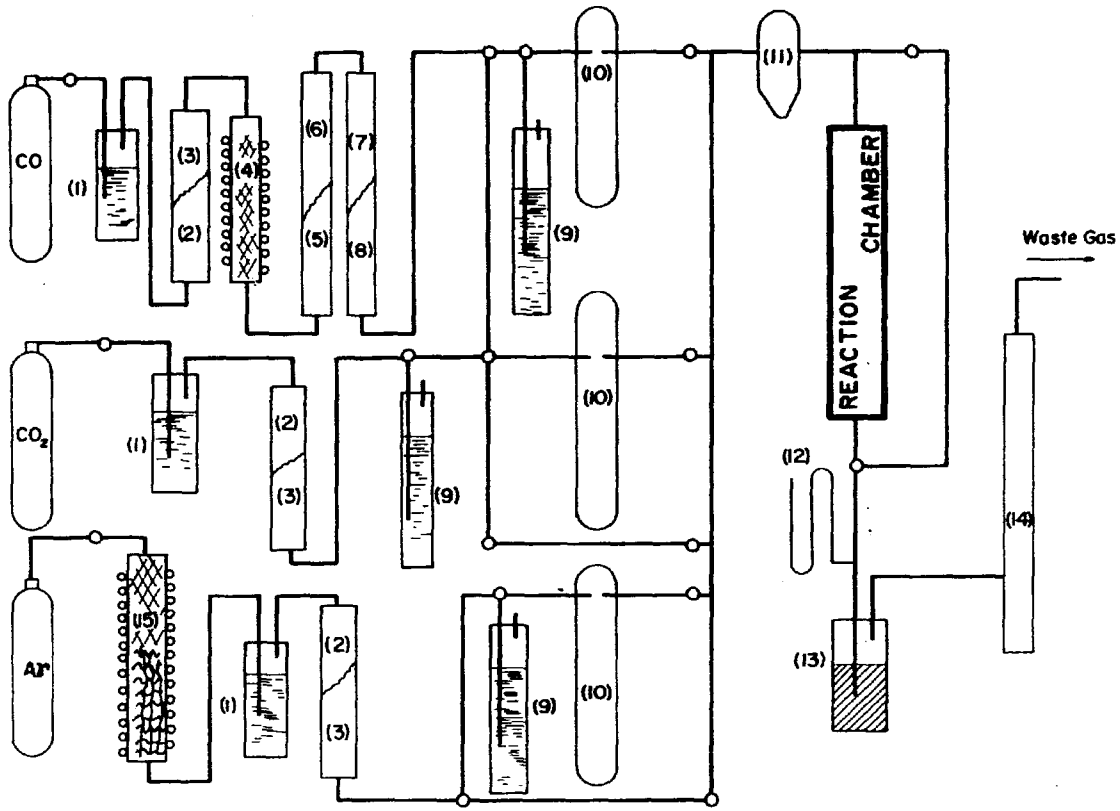

Fig. 1. Schematic Diagram of Experimental Apparatus

Photo. 1. General View of the Experimental Apparatus.

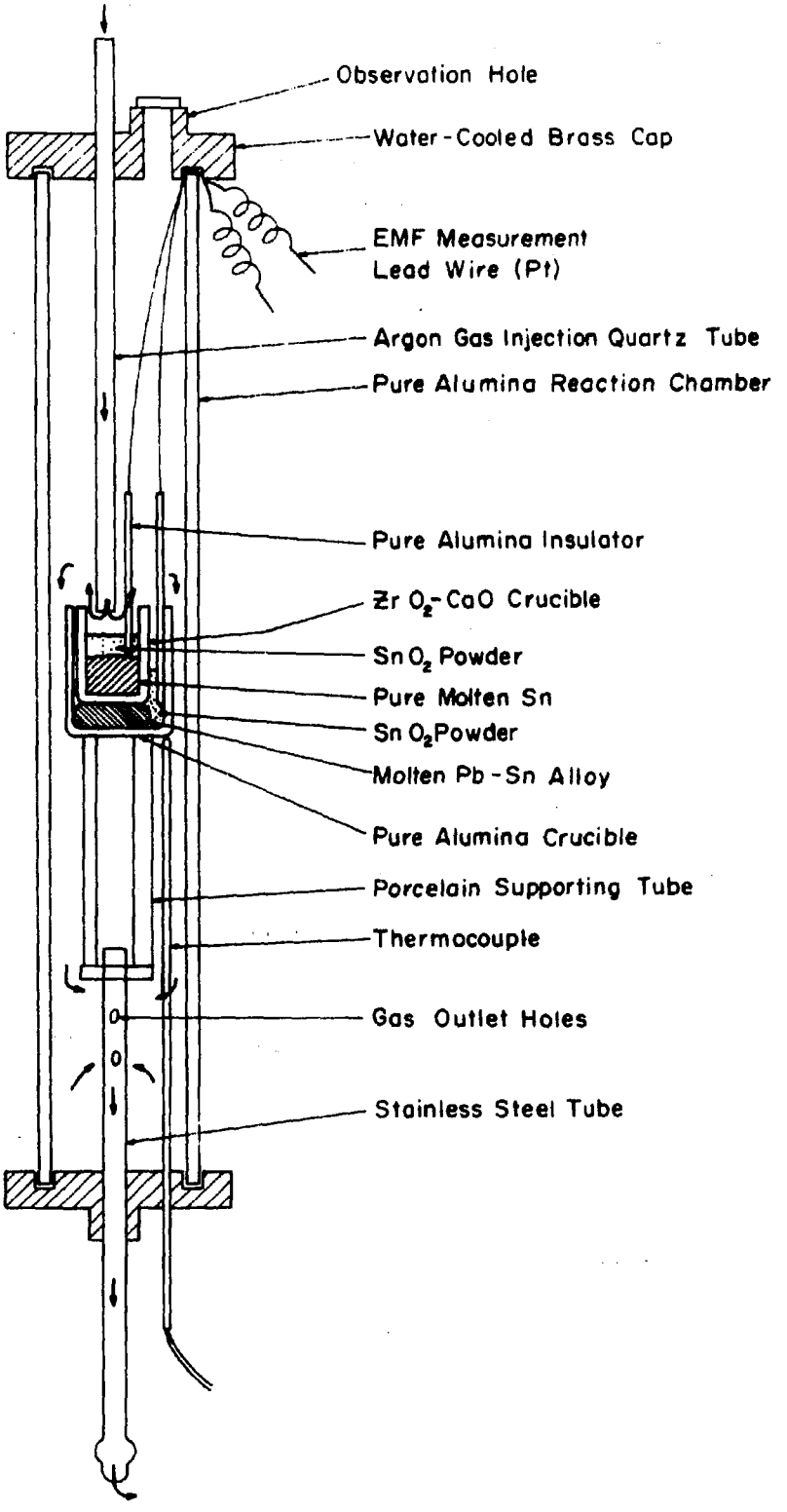

Fig. 2. Schematic Diagram of Reaction Chamber

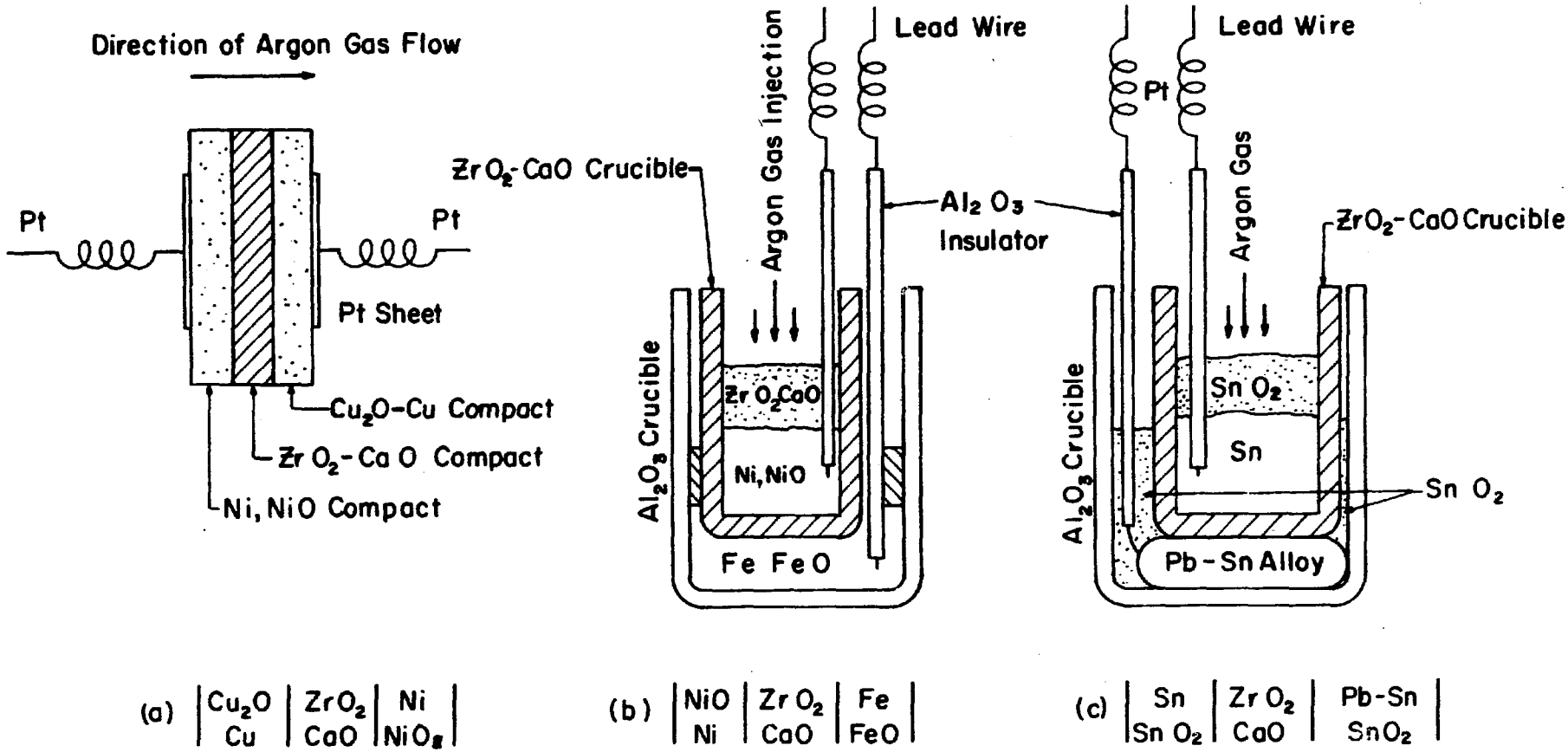

Fig. 3. Three Types of Oxygen Concentration Cells.

the inside diameter of the alumina crucible. The two crucibles were then assembled as shown in Figure 3. The lead wire was nichrome, covered with alumina insulators, which is stable in the presence of Ni and Fe powder.

For the | Pb • PbO | ZrO_2 - CaO | Sn • SnO_2 | cell, a similar arrangement was used as in the case of | FeO • Fe | ZrO_2 - CaO | Ni - NiO | cell. However, the lead and tin were in a granulated state and the lead wire was platinum which is stable in the presence of Pb and Sn. The lead and tin forms a homogeneous melt at the experimental temperature.

The cell was set into the reaction chamber. The electric power of the furnace was turned on after flushing in the reaction chamber with argon gas passed through the cleaning train. The cells were kept at a given temperature for 1 to 2 hours to attain equilibrium at both electrodes. When the EMF stabilized, both the temperature and the EMF were read with the potentiometers several times.

Results of the Experiments

The results of the EMF measurements are given in Tables 1, 2, and 3 for the three different types of oxygen concentration cells. The measured EMF is the difference of the standard free energy of formation of the oxides at both electrodes. Therefore, the EMF gives this difference by the equation

$$\Delta F^{\circ} = -nE\mathcal{F} \qquad (15)$$

The ΔF°'s are shown in Figures 4, 5, and 6. In the figures, ΔF°, the standard free energy calculated from Elliot and Gleiser's data[1] of the

standard free energy of formation of metal oxides, is shown for comparison. The present results agreed with them within 0.5 K cal.

From these figures, the following ΔF° values are obtained:

$$NiO + 2Cu = Cu_2O + Ni \qquad (16)$$

$$\Delta F^{\circ} = 15{,}400 - 2.870\ T\ (^{\circ}K)\ (700^{\circ} - 1050^{\circ}C) \qquad (17)$$

$$FeO + Ni = NiO + Fe \qquad (18)$$

$$\Delta F^{\circ} = 5{,}280 + 5.88\ T\ (^{\circ}K)\ (700^{\circ} - 1200^{\circ}C) \qquad (19)$$

$$\tfrac{1}{2}SnO_2 + Pb = PbO + \tfrac{1}{2}Sn \qquad (20)$$

$$\Delta F^{\circ} = 15{,}550 - 0.150\ T\ (^{\circ}K)\ (600^{\circ} - 850^{\circ}C) \qquad (21)$$

The standard free energies of formation of the oxides may not be presented here with the limited number of experiments. The free energies of the above reactions agree with the calculated values,[1] if the accuracies of the standard free energies of formation[1] of FeO, NiO, Cu_2O, SnO_2, and PbO are considered which are 47,550 cal, 35,910 cal, 23,300 cal, 89,150 cal and 28,750 cal, respectively, at 1000°K.

The free energy of the formation of wustite is based upon the investigations by Humphrey, King, and Kellog,[8] Darken and Gurry,[9] Dingmann, Kirscht, and Wesselkack,[10] Gokcen,[11] and by Coughlin, King, and Bonnickson[12] and the accuracy is very good. However, the standard free energy of formation of Cu_2O based upon Kiukkola and Wagner[6] data differed by about 500 cal from the results obtained by the gas equilibrium measurements[1,15,16] which had a scatter of about 1000 cal.

The free energies of formation of PbO and SnO_2 are based on the tables by Coughlin[3] which may have much more inaccuracy than the above cases. Therefore, the deviation of less than 500 cal in the present results may not be considered to be significant.

Using the same method, Foster[4] measured the standard free energy of formation of tantalum oxides which also has some deviation from the calculated values. Therefore, there may be some type of polarization or some degree of electron conduction in these cells. Nevertheless, this fact is not significant for the present study in which absolute values of EMF are less important.

At the conclusion of the preliminary experiment, it was determined that the commercial stabilized zirconia works satisfactorily as an anion conductor.

TABLE 1. EMF MEASUREMENTS ON

$|Ni \cdot NiO|ZrO_2 - CaO|Cu_2O \cdot Cu|$ CELL

Temperature	EMF	ΔF°
773°C	269.8 mV	12,440 cal
763	270.7	12,480 cal
761	270.3	12,470 cal
764	269.9	12,450 cal
768	269.6	12,430 cal
835	263.7	12,160 cal
835	263.7	12,160 cal
835	263.8	12,160 cal
835	263.8	12,160 cal
835	263.8	12,170 cal
935	258.0	11,900 cal
940	257.7	11,880 cal
940	257.9	11,890 cal
940	257.9	11,890 cal
940	257.9	11,890 cal
1037	251.9	11,620 cal
1038	251.8	11,610 cal
1038	251.9	11,610 cal
1037	251.9	11,620 cal
1037	252.0	11,620 cal
1037	252.0	11,620 cal
1170	250.7	11,560 cal
1167	250.8	11,570 cal
1167	250.9	11,570 cal
1163	251.0	11,580 cal

TABLE 2. EMF MEASUREMENTS ON

| Fe • FeO | ZrO_2 - CaO | Ni • NiO | CELL

Temperature	EMF	ΔF°
700°C	235.4 mV	10,860 cal
700	235.9	10,880
700	236.0	10,880
700	236.0	10,880
803	255.5	11,780
800	255.3	11,770
800	255.4	11,780
800	255.3	11,770
800	255.7	11,780
894	268.2	12,370
896	268.2	12,370
897	268.6	12,390
898	268.7	12,390
897	268.7	12,390
897	268.6	12,380
987	271.7	12,530
987	272.6	12,570
987	271.7	12,530
1094	286.3	13,200
1094	286.6	13,220
1095	286.8	13,230
1095	286.9	13,230
1095	287.0	13,230
1194	301.2	13,890
1195	301.2	13,890
1195	301.2	13,890
1194	301.0	13,880

TABLE 3. EMF MEASUREMENTS ON

$| Sn \cdot SnO_2 | ZrO_2 - CaO | Pb \cdot PbO |$ CELL

Temperature	EMF	ΔF^o
778°C	334.6 mV	15,430 cal
778	334.8	15,440
778	334.7	15,440
778	334.9	15,440
778	335.0	15,450
721	335.0	15,450
721	335.0	15,450
721	335.1	15,450
721	334.9	15,440
670	333.3	15,370
670	333.1	15,360
670	333.1	15,360
670	332.9	15,350
620	331.8	15,300
622	331.9	15,310
622	331.9	15,310
622	331.8	15,300
842	332.1	15,310
842	332.1	15,360
842	332.2	15,320
842	331.8	15,300

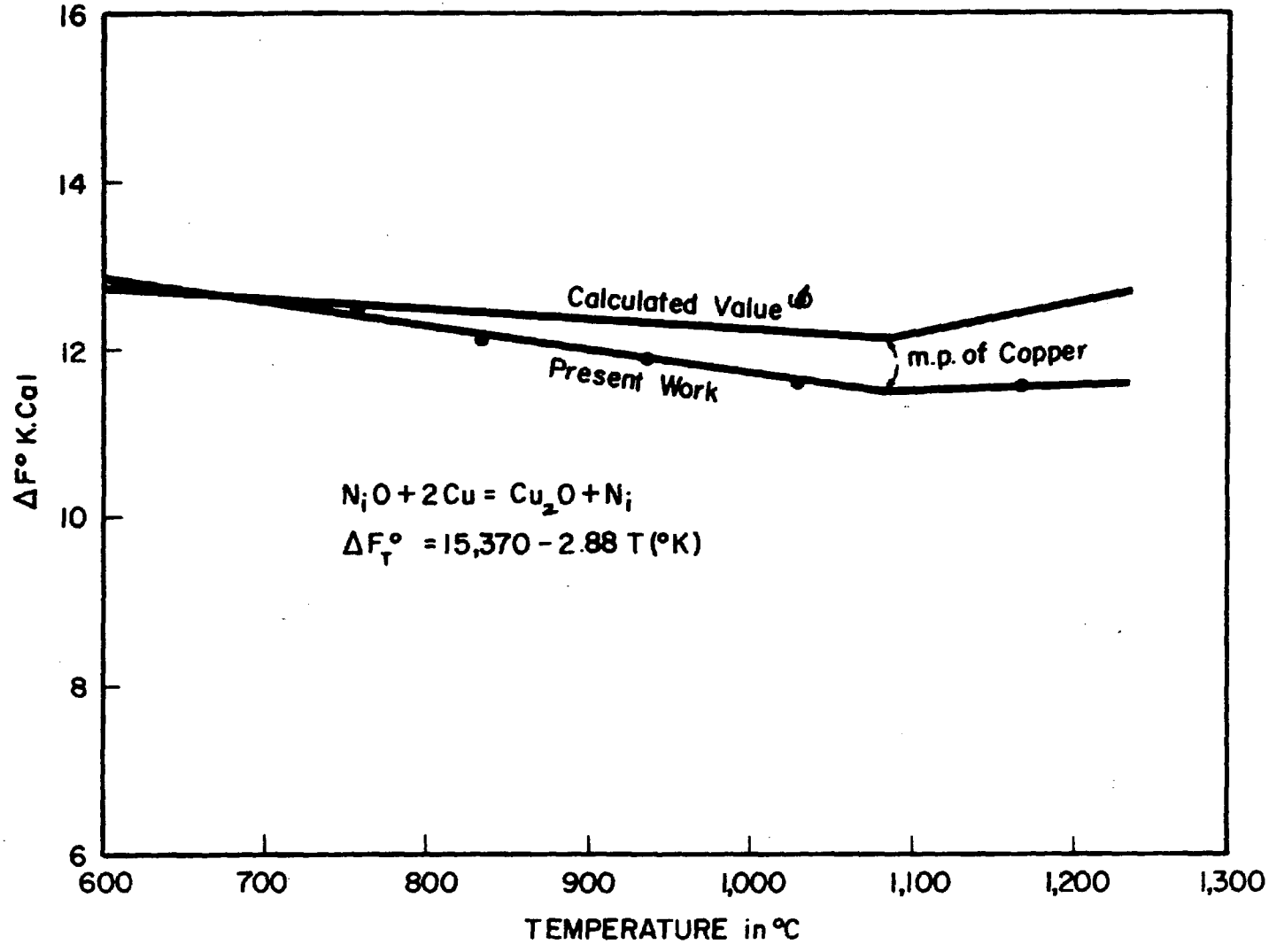

Fig. 4. Free Energy Change of the Reaction of NiO + 2Cu = Cu_2O + Ni.

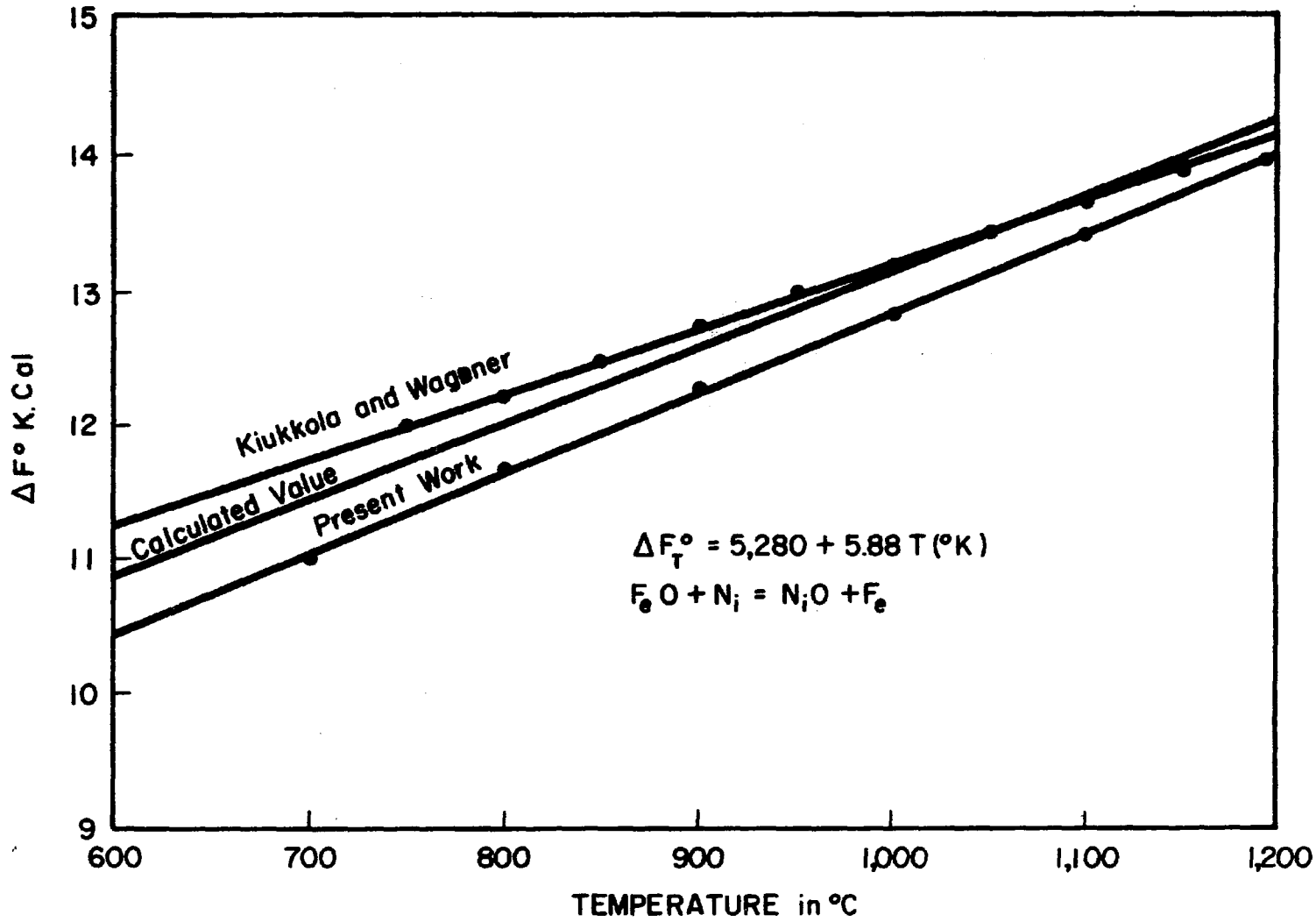

Fig. 5. Free Energy Change of the Reaction: FeO + Ni = NiO + Fe.

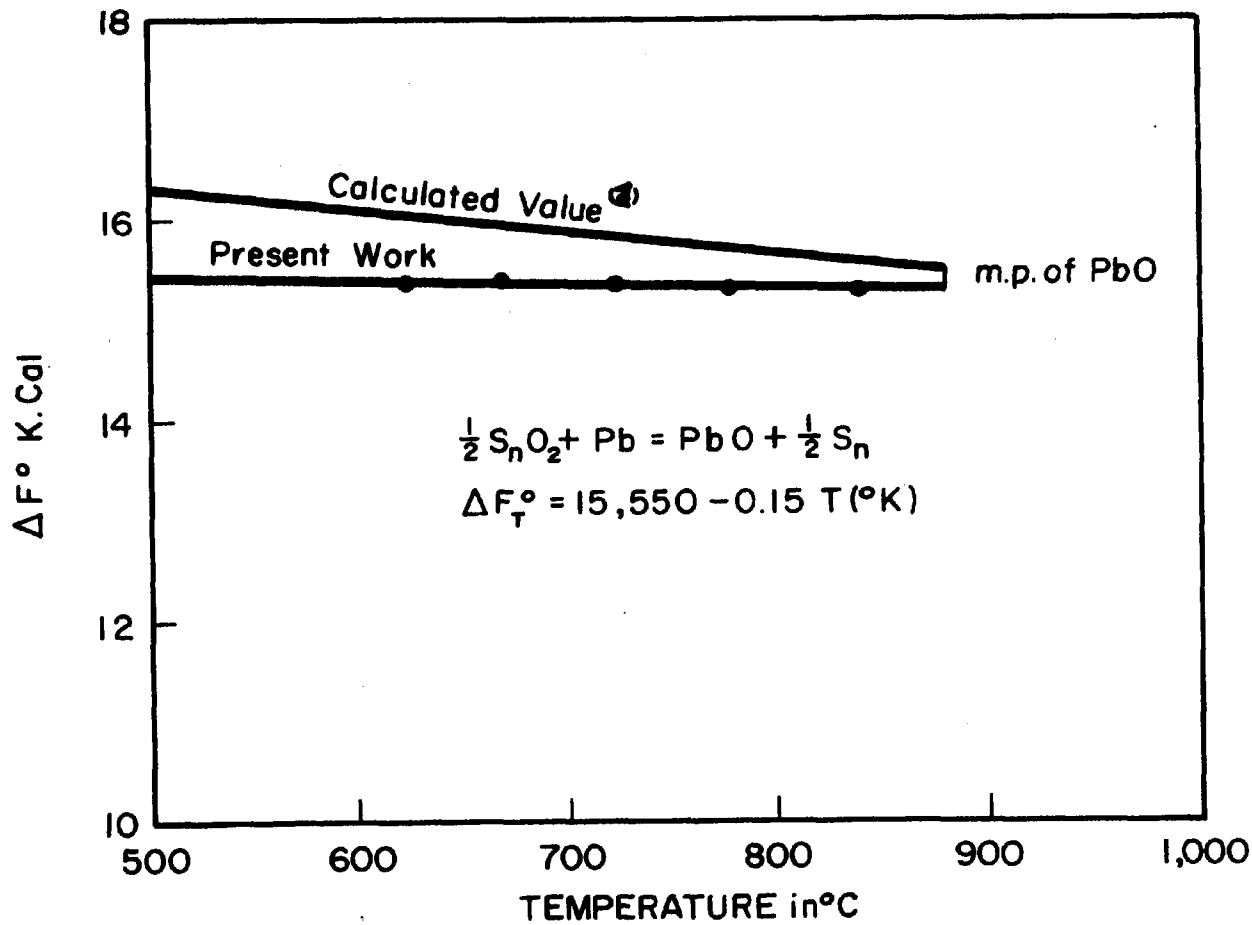

Fig. 6. Free Energy Change of the Reaction: $\frac{1}{2}SnO_2 + Pb = PbO + \frac{1}{2}Sn$.

CHAPTER II

ACTIVITY MEASUREMENTS OF LIQUID LEAD-TIN ALLOYS

Synopsis

The activity of tin has been measured at 700°C, 800°C, and 900°C by the oxygen concentration cell technique. The activity of tin deviates in a positive direction from ideality, with the deviation increasing with decreasing temperature. The activity of lead was obtained by the Gibbs-Duhem equation and also shows a positive deviation from ideality. The free energy of solution of the lead-tin system as well as the excess free energy of solution was calculated. Also, the partial molal free energies of lead and tin were calculated.

Experimental Apparatus

The details of the experimental apparatus have already been shown in the previous chapter. However, a quartz tube was used to inject the oxygen-free argon gas onto the crucible combination to prevent mixing with the electrode atmosphere.

Figure 3(c) shows the cell assembly, in which pure tin metal and tin-lead alloy are separated by the zirconia crucible.

Preparation of Cells and Experimental Procedure

For the activity measurement of tin in molten lead-tin alloys, 20.000 gm of lead and tin mixture were pressed into a tablet 1.0 inch in diameter and then set into the alumina crucible. The cell was

$|Pb - Sn$ alloy $\cdot SnO_2|\ ZrO_2 - CaO\ |Sn \cdot SnO_2|$. The pressing of the lead-tin mixture into a tablet was necessary to obtain a homogeneous melt at the experimental temperature.

The cell was set into the reaction chamber. The electric power was turned on to heat the cell after flushing out the air in the chamber with oxygen-free argon gas. When both the temperature and EMF were stabilized, they were measured several times by the potentiometers.

After cooling, the lead-tin alloys were chemically analyzed by the standard method of ASTM, E46-56 (tin analysis by the iodimetric titration method). Accuracy of the tin analyses was $\pm 0.3\%$.

Some of the experimental runs were carried out in a crucible made by the author from zirconyl nitrate to compare the performances of the commercial crucibles with the home-made pure zirconia-lime crucibles. The procedure for preparing the pure ZrO_2 - CaO crucible was as follows:

1. Mixing of $ZrO(NO_3)_2$ solution (20%) and dilute nitric acid solution of $CaCO_3$.
2. Drying in a water bath and heating at 120°C for two nights to decompose the $ZrO(NO_3)_2$ and volatilize NO_2 gas.
3. Sintering at 1350° to 1400°C for two days.
4. Pressing the sintered powder to a 1.0 inch diameter block under 15,000 psi.
5. Boring the block with a drill to form the cavity and finishing into a crucible shape.
6. Sintering the crucible at 1500° to 1700° C in a high frequency induction furnace under a reducing atmosphere for 3 hours.
7. Sintering the crucible at 800° to 900°C for 1 to 2 hours in an oxidizing atmosphere to oxidize the adsorbed carbon.

Results of the Experiment

The results of the activity measurement are shown in Figures 7, 8, and 9 at 700°C, 800°C, and 900°C, respectively, and also in Tables 4, 5, and 6.

Figures 10 and 11, respectively, show the free energy of mixing and the excess free energy of mixing of lead and tin. Figures 12 and 13 show the molal free energy of lead and tin and the molal excess free energy of lead and tin. The activity of both the lead and tin deviate in a positive direction from ideality and the degree of the deviation increased with decreasing temperature. The free energy of solution of the Pb - Sn system was calculated by the equation:

$$\Delta F^{mix} = RT(N_{Pb}\ln a_{Pb} + N_{Sn}\ln a_{Sn}) \qquad (22)$$

The excess free energy of the solution was calculated by

$$\Delta F^{excess} = RT(N_{Pb}\ln \gamma_{Pb} + N_{Sn}\ln \gamma_{Sn}) \qquad (23)$$

Discussion of the Results

As shown in Figure 14, the so-called α plot in the Gibbs-Duhem integration was scattering very much because the activity coefficient of tin is very close to unity in the present results. This means that any small fluctuation of the γ_{Sn} (activity coefficient) value results in a very large deviation in the α plot as shown below.

$$\alpha_{Sn} = \frac{\ln \gamma_{Sn}}{N_{Pb}^2} \doteqdot \frac{\gamma_{Sn} - 1}{N_{Pb}^2} \text{ because } \ln(1+\varepsilon) \doteqdot \varepsilon$$

$$\text{if } \varepsilon \ll 1. \qquad (24)$$

TABLE 4. ACTIVITY MEASUREMENTS OF Pb - Sn SYSTEM AT 700°C

Run No.	N_{Sn}	EMF (mV)	a_{Sn}	γ_{Sn}
10	0.7347	8.89	0.795	1.082
12	0.5877	14.9	0.701	1.193
13	0.2953	34.1	0.443	1.501
16	0.1429	49.1	0.310	2.167
17	0.7236	10.3	0.783	1.082
21	0.07108	72.2	0.179	2.517
24	0.1622	48.9	0.310	1.913
30*	0.1627	49.0	0.309	1.900
31*	0.3059	34.2	0.441	1.441
32*	0.4232	24.1	0.562	1.329
33*	0.5905	13.9	0.718	1.215
35*	0.1615	43.3	0.355	2.195
40	0.6349	11.9	0.752	1.184
41	0.7183	9.0	0.806	1.123
42	0.8035	7.7	0.832	1.036

*For these runs, the pure ZrO_2 - CaO crucibles, which have been made by the author, were used.

TABLE 5. ACTIVITY MEASUREMENTS OF Pb - Sn SYSTEM AT 800°C

Run No.	N_{Sn}	EMF (mV)	a_{Sn}	γ_{Sn}
12	0.5347	21.1	0.620	1.160
13	0.2953	42.1	0.402	1.362
15	0.7665	11.7	0.777	1.014
16	0.1429	68.7	0.227	1.585
17	0.7236	12.5	0.783	1.053
18	0.4282	32.2	0.498	1.164
19	0.8401	7.5	0.849	1.010
20	0.6214	17.4	0.686	1.104
21	0.07108	84.7	0.160	2.255
23	0.1625	68.2	0.229	1.407
24	0.1622	68.3	0.228	1.406
32*	0.4232	32.1	0.500	1.181
35*	0.1615	66.8	0.236	1.460
40	0.6349	16.2	0.704	1.108
41	0.7183	12.2	0.768	1.069
42	0.8035	8.5	0.832	1.035

TABLE 6. ACTIVITY MEASUREMENTS OF Pb - Sn SYSTEM AT 900° C

Run No.	N_{Sn}	EMF (mV)	a_{Sn}	γ_{Sn}
36	0.1597	87.0	0.179	1.121
37	0.3006	53.3	0.348	1.159
38	0.4205	38.4	0.468	1.112
39	0.5427	27.5	0.580	1.069
40	0.6349	22.1	0.646	1.018
41	0.7183	15.2	0.740	1.030
42	0.8035	10.3	0.816	1.016

$$d\alpha_{Sn} = \frac{1}{N_{Pb}^2} \cdot \frac{d\gamma_{Sn}}{\gamma_{Sn}} - \ln \gamma_{Sn} \frac{2dN_{Pb}}{N_{Pb}^3} \qquad (25)$$

$$\left| \frac{d\alpha_{Sn}}{\alpha_{Sn}} \right| = \frac{d\gamma_{Sn}}{\gamma_{Sn} \ln \gamma_{Sn}} - 2 \frac{dN_{Pb}}{N_{Pb}} \qquad (26)$$

$$\left| \frac{d\alpha_{Sn}}{\alpha_{Sn}} \right| \doteq \left| \frac{d\gamma_{Sn}}{\gamma_{Sn}(\gamma_{Sn} - 1)} \right| + 2 \left| \frac{dN_{Pb}}{N_{Pb}} \right|$$

$$\text{for } \gamma_{Sn} \doteq 1.0 \qquad (27)$$

For example, $\gamma_{Sn} = 1.05$, $d\gamma_{Sn} = 0.02$ and $\frac{dN_{Pb}}{N_{Pb}} = 0.05$ results in

$$\left| \frac{d\alpha_{Sn}}{\alpha_{Sn}} \right| = 0.4 + 0.1 = 0.5 \qquad (28)$$

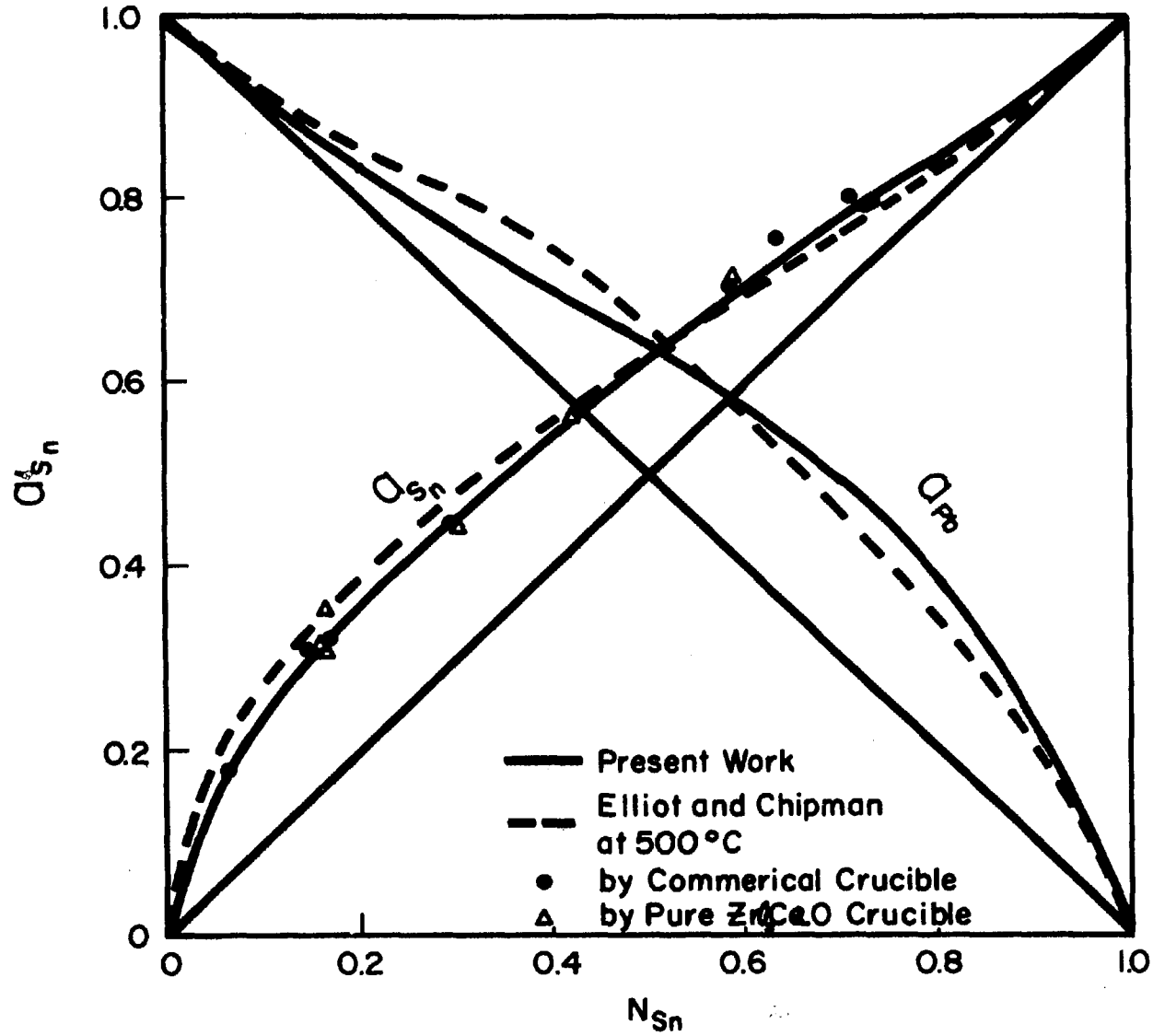

Fig. 7. Activity of Sn vs. N_{Sn} at 700°C.

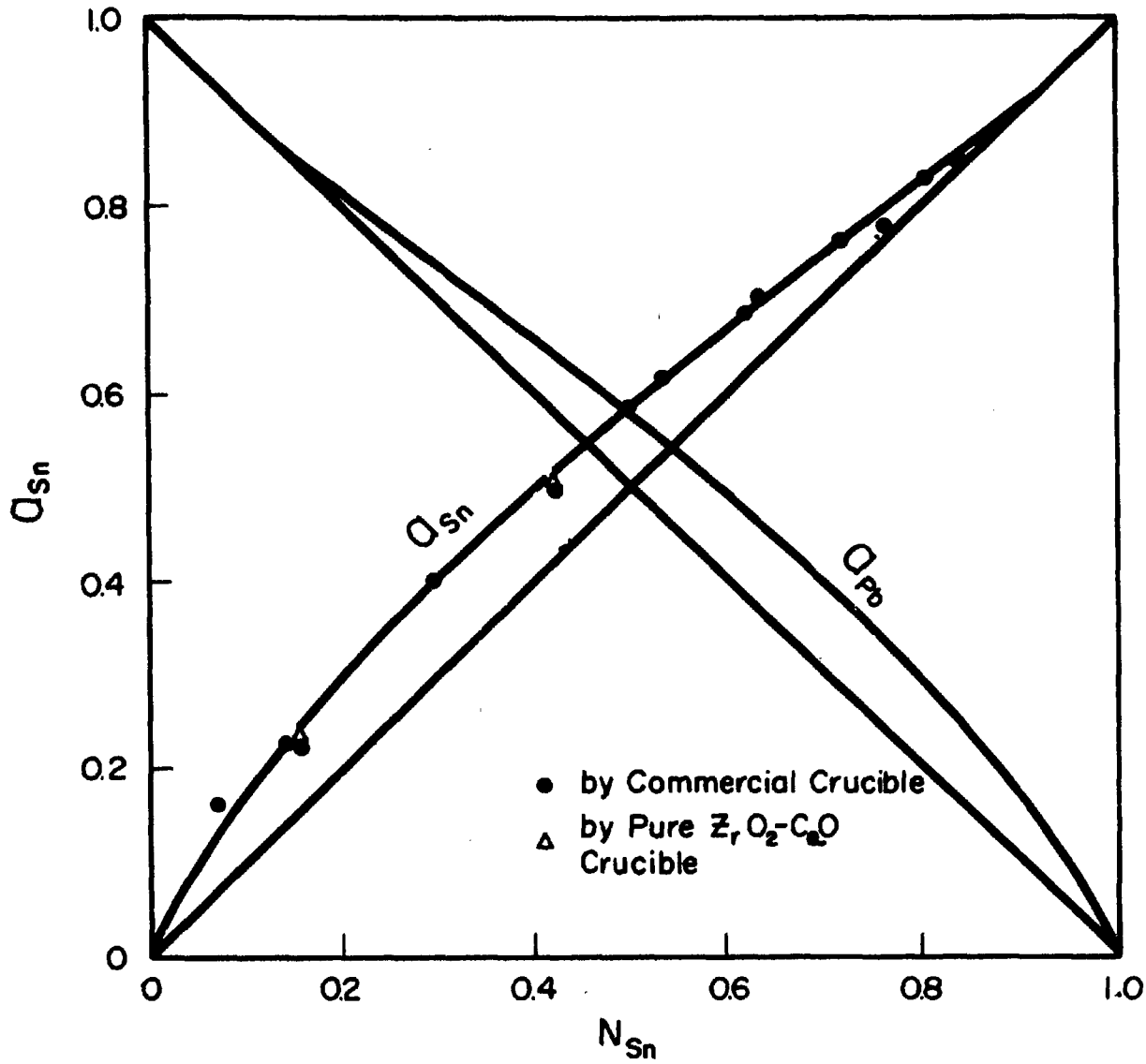

Fig. 8. Activity of Sn vs. N_{Sn} at 800°C.

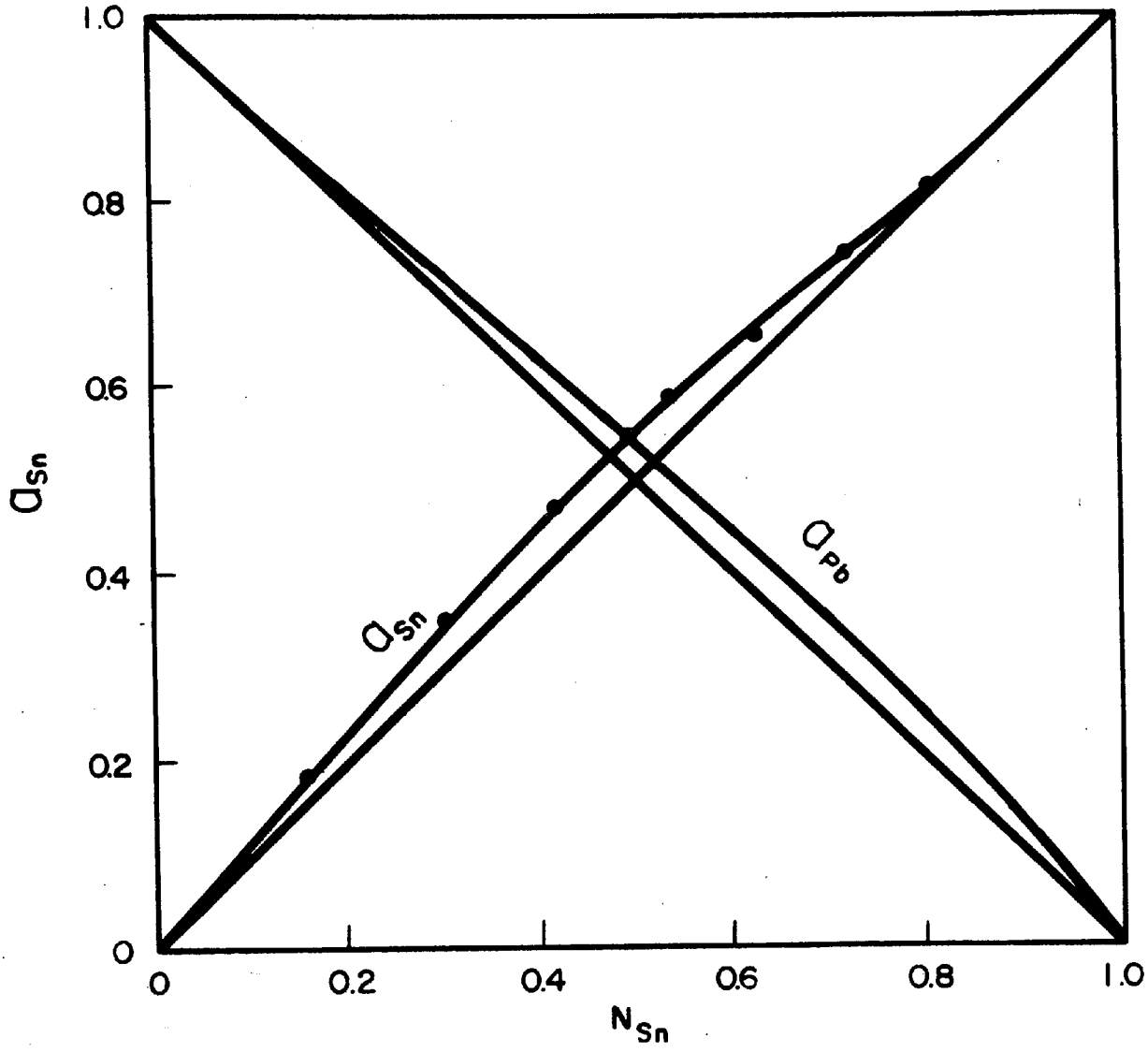

Fig. 9. Activity of Sn vs. N_{Sn} at 900°C.

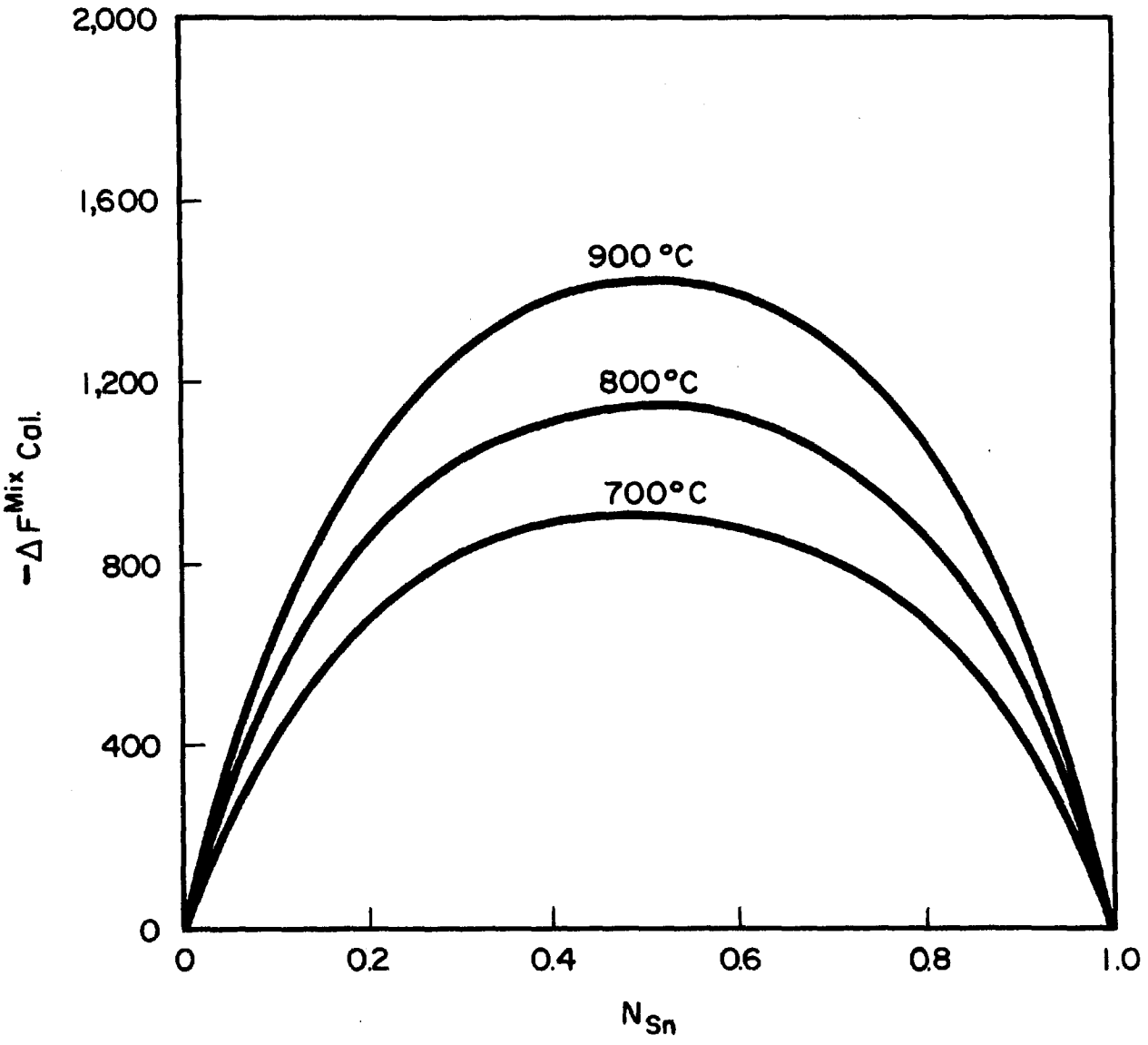

Fig. 10. Free Energy of Mixing of Pb-Sn Alloys.

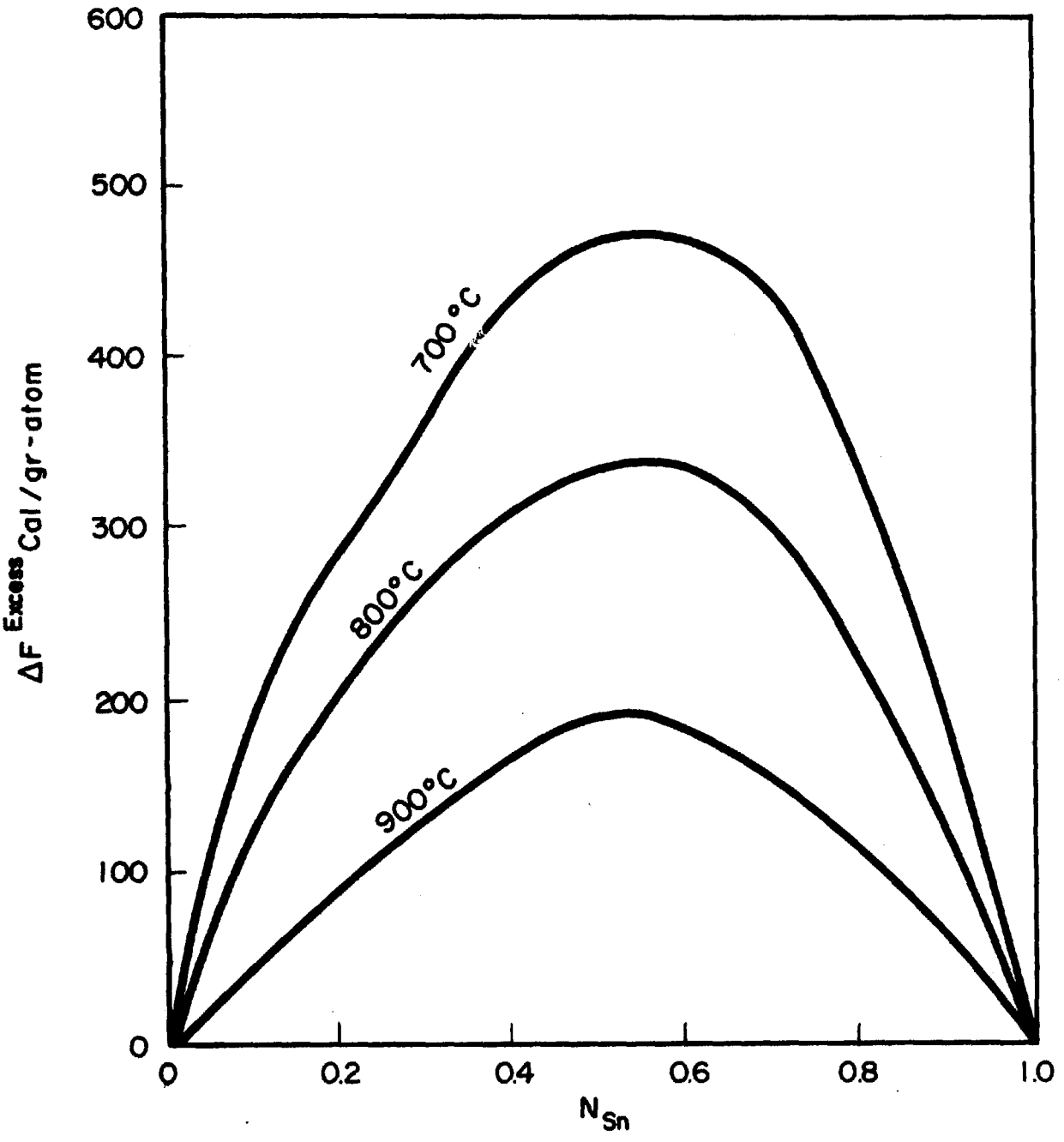

Fig. 11. Excess Free Energy of Mixing of Pb-Sn Alloys.

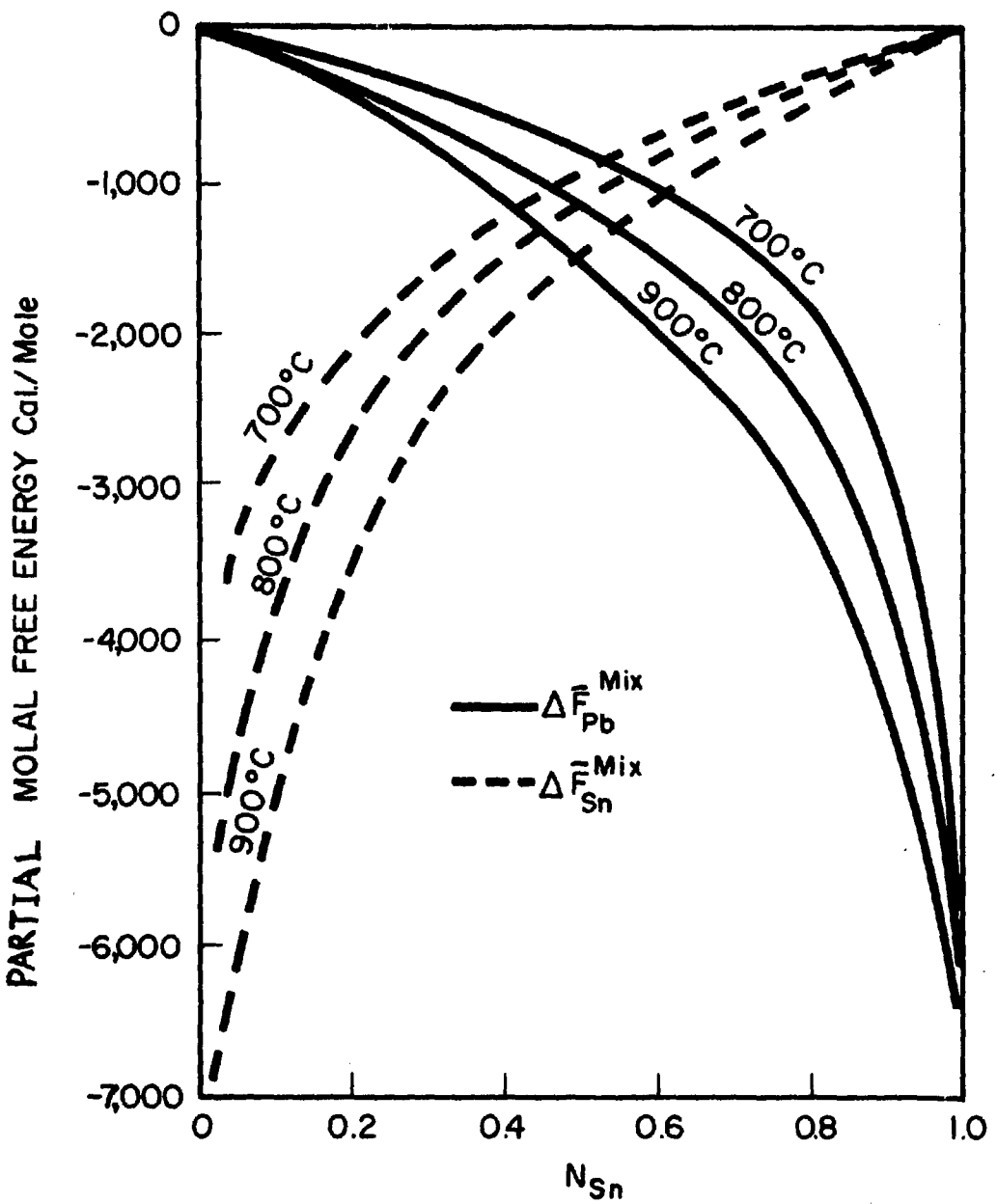

Fig. 12. Partial Molal Free Energy of Pb and Sn.

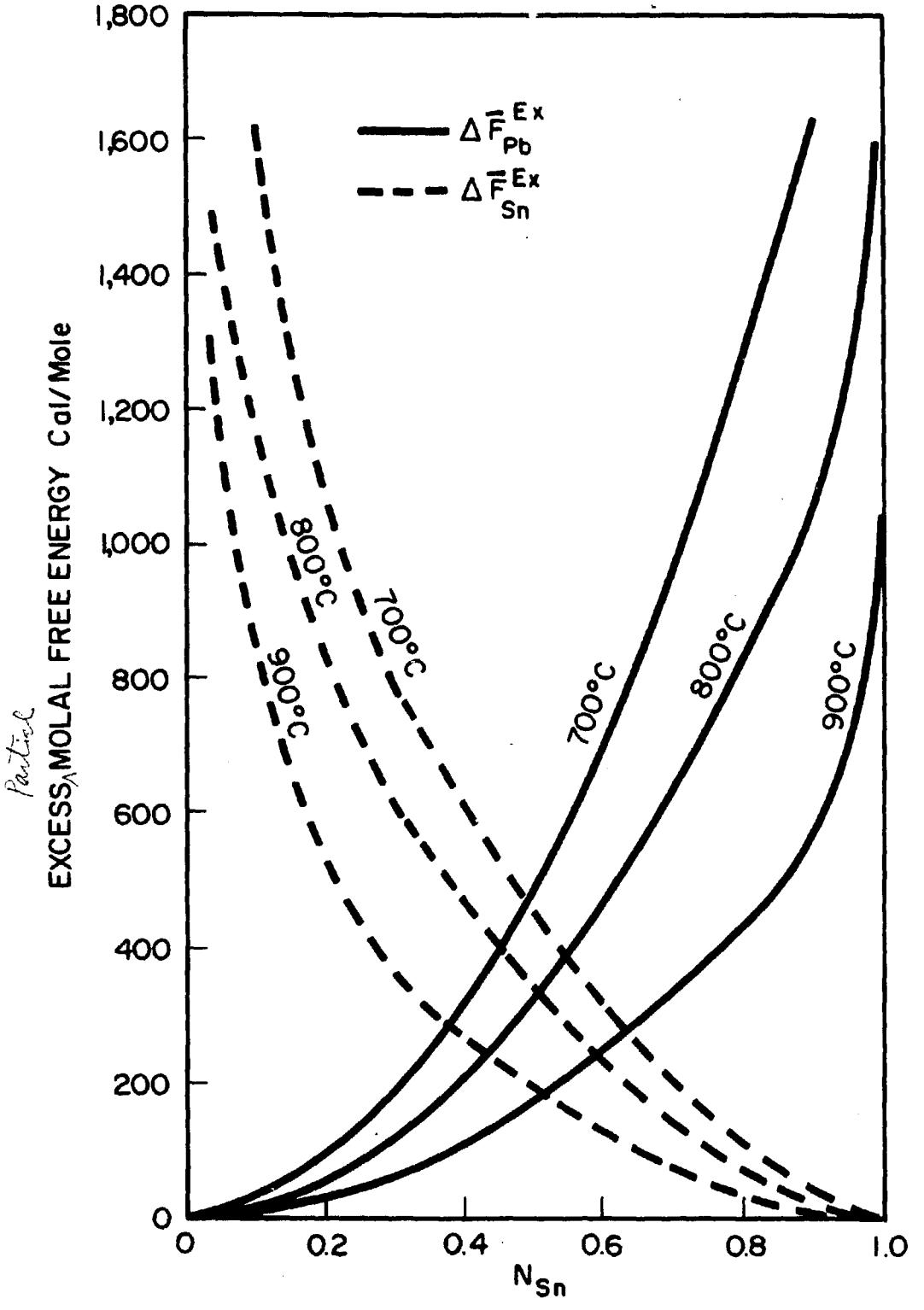

Fig. 13. Excess Partial Molal Free Energy of Pb and Sn.

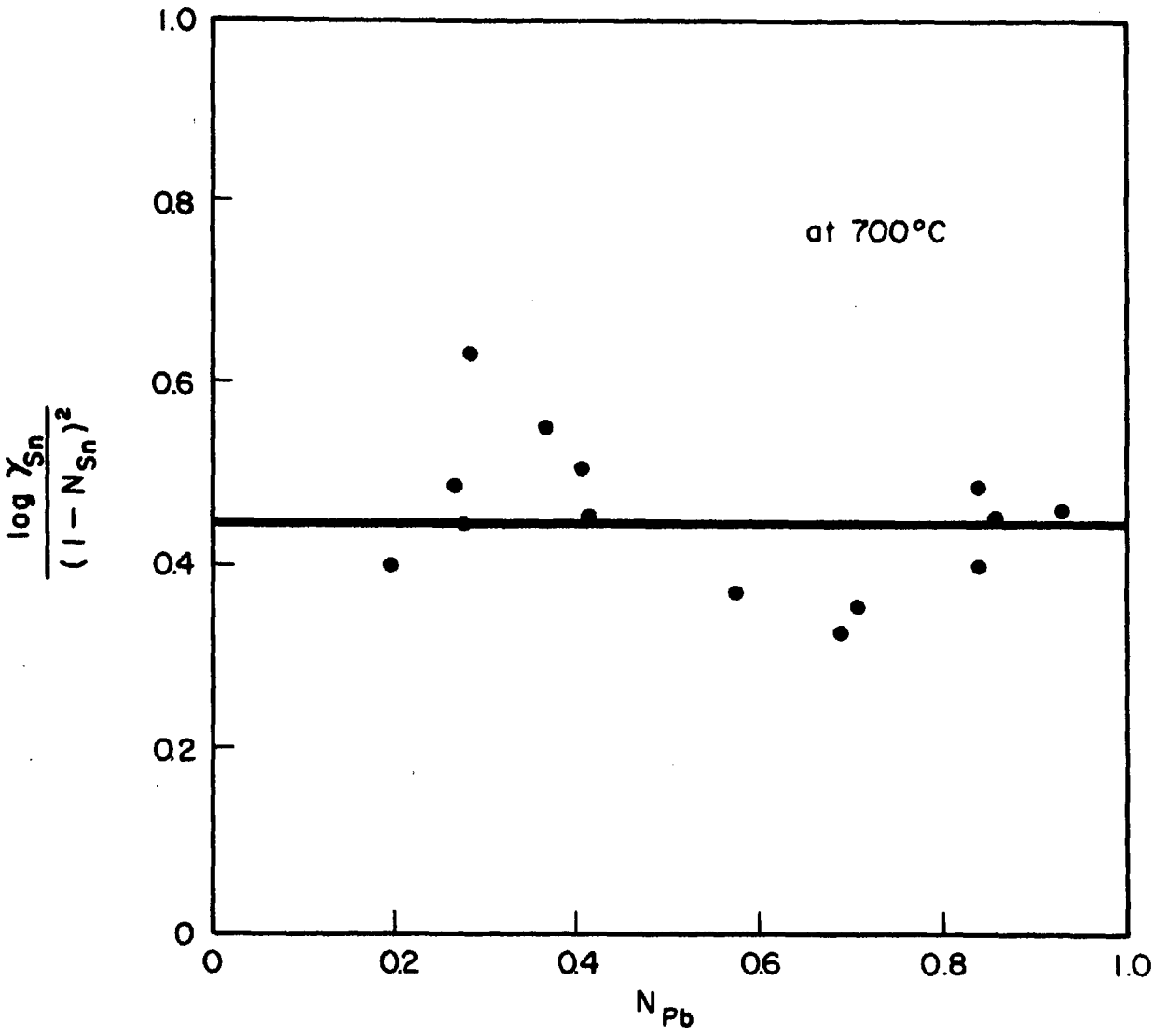

Fig. 14. Relationships between log $\gamma_{Sn}/(1-N_{Sn})^2$ and N_{Pb}.

The previous statements result in the inherent inaccuracy of the calculation of the activity of lead. No activity data are available on the lead tin system except the calculated value from the Pb-Sn-Cd ternary data by Elliott and Chipman.[18] The calculated activity of lead and tin by Elliott and Chipman is shown by the broken lines in Figure 7.

In general, the Gibbs-Duhem calculation of a ternary solution is very inaccurate; therefore, results calculated by Eliott and Chipman may be incorrect. Nevertheless, their calculated activity seems to agree with the present data, although the experimental temperature is different by about 200°C.

In order to determine whether the lead-tin alloy is a regular solution or not, the following conditions should be considered.

1. Whether α is constant at a given temperature for any composition of alloy.
2. Whether the following relation is satisfied.

$$\left(\frac{d\alpha}{d\, 1/T}\right)_{PN_1N_2} - T\alpha = 0 \qquad (29)$$

Both of the above conditions should be satisfied for a regular solution. The present system seems to satisfy condition (1) but not (2), and it can be concluded that the lead-tin solution is not a regular solution, although the free energy of mixing seems almost symmetrical at $N_{Pb} = N_{Sn} = 0.5$. The second condition can be derived easily from the definition of the regular solution where the entropy of mixing is ideal and heat of mixing is independent of temperature.

$$\Delta F^{Mix} = \Delta H^{M} - T\Delta S^{M} \tag{30}$$

$$\ln \gamma_1 = \alpha N_2^2, \quad \ln \gamma_2 = \alpha N_1^2 \tag{31}$$

$$\Delta F^{Mix} = RT\left[N_1 N_2 \alpha + N_1 \ln N_1 + N_2 \ln N_2 \right] \tag{32}$$

$$H^{M}_{N_1 N_2 P} = \left(\frac{dF^{M}/T}{d\ 1/T}\right)_{P, N_1 N_2} \tag{33}$$

$$= \frac{d}{d\ 1/T}\left[R(\alpha N_1 N_2 + N_1 \ln N_1 + N_2 \ln N_2) \right]_{P N_1 N_2} \tag{34}$$

$$= RT\alpha N_1 N_2 \tag{35}$$

$$RN_1 N_2 \left(\frac{d\alpha}{d\ 1/T}\right)_{P N_1 N_2} - RT\alpha N_1 N_2 = 0 \tag{36}$$

The effect of oxygen in lead-tin alloys on the activity of tin or lead is assumed to be negligible, because the solubility of oxygen in liquid lead has been determined by Alcock[19] to be about 0.13 atomic % at 700°C, using the coulombmetric titrations. Thus, the effect of the oxygen on the activity of tin is assumed to be negligible.

The vapor pressure of tin is rather large (10^{-4} atm at 692°C and 10^{-3} atm at 809°C), therefore, the final tin content in Pb-Sn alloys was decreased from the charge composition.

The EMF was very sensitive to the atmosphere over the cell. If pure CO or CO_2 was mixed with the argon atmosphere, the EMF spontaneously decreased or increased; and if pure argon flowed over the cell, the EMF returned to the original reversible EMF value in a short time.

In addition, four zirconia crucibles of different sizes have been used and one of them was made by the present author as described above. The EMF obtained was constant regardless of the difference in the size of the crucibles. This implies that the effect of mixing of both

electrode atmospheres on the EMF is negligible in the present activity measurement.

From the above considerations, the author believes that the present results give the accurate activity of tin in liquid lead-tin alloys. The fluctuation of the EMF was less than $\pm$ mV.

To study the mobility of oxygen through the electrolyte, the polarization, and the possibility of coulombmetric titration, the following cell was constructed.

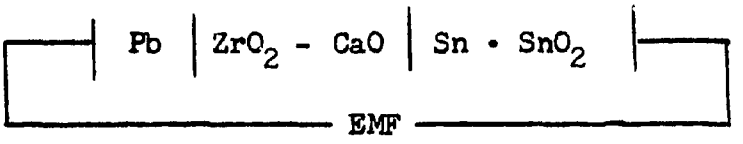

After homogenization of the cell, an external potential of 0 to 900 mV was applied at 628°C, and the current was measured. The results of these measurements are given in Figure 15.

From these measurements, the reversible EMF is determined at zero current and is reversible with respect to the applied potentials. The reversible EMF was 238.8 mV by the Galvanometer and 243.7 mV by the microammeter.

The slope of the current vs. the applied potential curve gives the mobility of oxygen through the electrolyte, and the empirical resistivity[21,22] of the cell, which is about $4.59 \times 10^4 \Omega$ at 628°C. The cell current at the reversible EMF at 628°C was 5.90 μA and did not go to zero due to polarization, showing polarization was not existent at the reversible EMF.

From these results, it was shown that the EMF is reversible with respect to the applied potential and there is no polarization at the reversible EMF.

Then, an external potential of 2 volts was applied to pump out the oxygen in liquid lead or pump in oxygen into liquid lead from the tin electrode side to study the possibility of the coulombmetric titration at $710^{\circ}C \pm 5^{\circ}$. However, the quantitative coulombmetric titration was not successful because the oxygen pressure over the liquid lead could not be controlled.

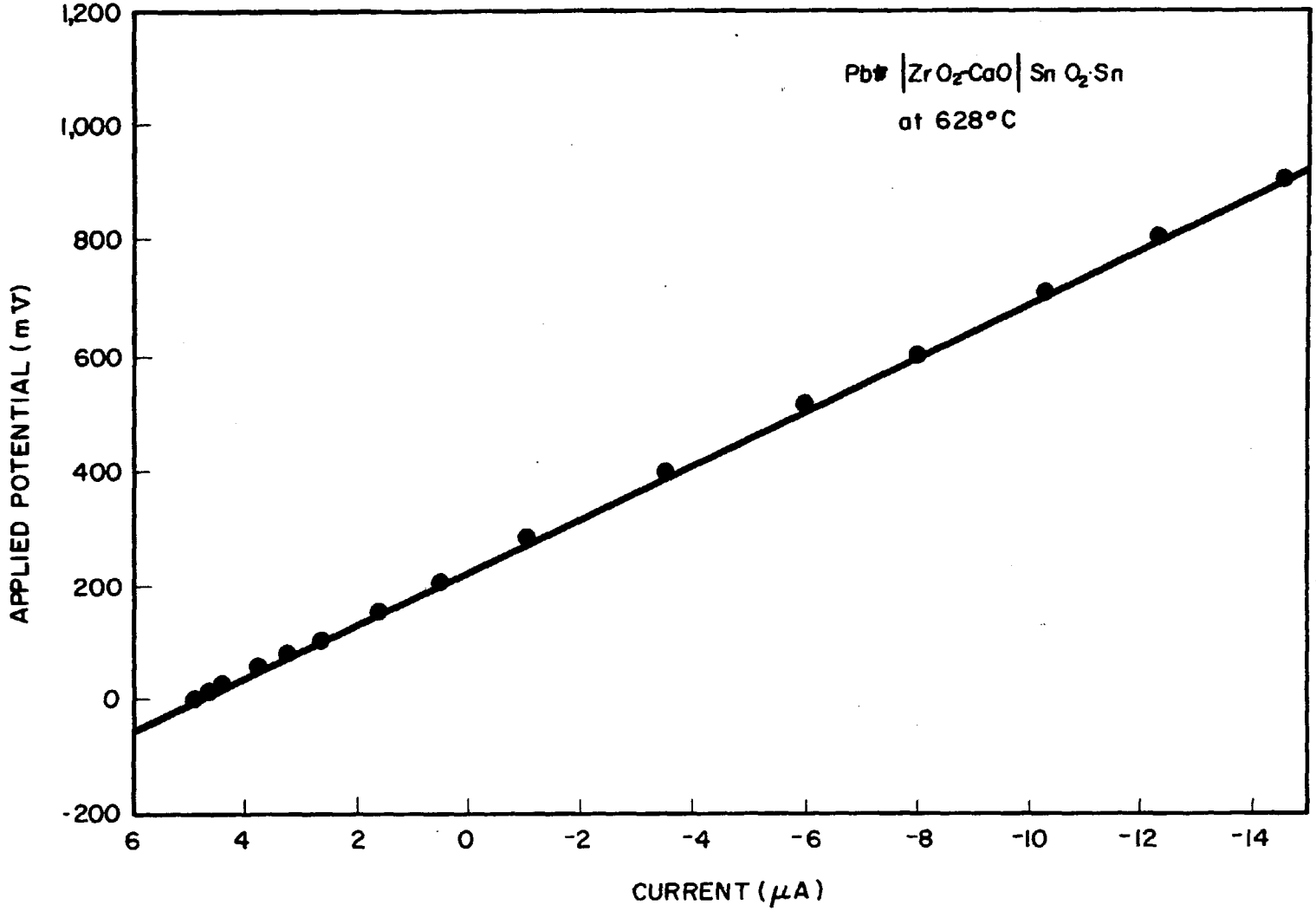

Fig. 15. Relationship between the Applied Potential and Current of the Cell: Pb $|ZrO_2 - CaO|\ SnO_2 \cdot Sn$.

CHAPTER III

DIRECT MEASUREMENTS OF THE PARTIAL PRESSURE OF OXYGEN IN HIGH TEMPERATURE GASES

Synopsis

The partial pressure of oxygen in carbon monoxide-carbon dioxide and argon-oxygen have been measured at temperatures of 800°C, 900°C, 1000°C, 1100°C and 1200°C by an oxygen concentration cell method. The cells employed are shown below:

1. $CO \cdot CO_2 \,\vdots\, FeO \cdot Pt \mid ZrO_2 - CaO \mid FeO \cdot Fe \mid Pt$ (EMF)

2. $CO \cdot CO_2 \,\vdots\, Pt \mid ZrO_2 - CaO \mid Ni \cdot NiO \mid Pt$ (EMF)

3. $CO \cdot CO_2 \,\vdots\, FeO \cdot Pt \mid ZrO_2 - CaO \mid Cu \cdot Cu_2O \mid Pt$ (EMF)

4. $\text{Air or } Ar + O_2 \,\vdots\, Pt \mid ZrO_2 - CaO \mid Ni \cdot NiO \mid Pt$ (EMF)

It was shown that this method is very convenient in analyzing directly the gas composition of CO and CO_2, or Ar and O_2 at the elevated temperatures as well as of other gas mixtures. Calibration curves of EMF against gas composition are presented.

Introduction

In the present chapter, it is shown that the oxygen concentration cells with the solid electrolyte of ZrO_2 - CaO and with the reference electrode of a powdered mixture of a pure metal and its oxide can be used as a convenient method of analyzing directly the composition of gases which have a fixed oxygen pressure at the temperature range of 800° to 1200°C. The principle of the present method is given by the following equation:

$$\Delta F = -n\mathcal{F}E = \frac{RT}{2} \ln \frac{P_{O_2}^{right}}{P_{O_2}^{left}} \tag{37}$$

for the reaction:

$$O_{left} \text{ (in Pt electrode)} = O_{right} \text{ (in Fe • FeO reference electrode)} \tag{38}$$

for

$$\begin{matrix} CO \\ \vdots \\ CO_2 \end{matrix} \vdots \; FeO \cdot Pt \;|\; ZrO_2 \cdot CaO \;|\; Fe \cdot FeO \;|\; Pt$$

(EMF)

Therefore, the difference in the partial pressure of oxygen at the cathode and the anode simply results in an electromotive force according to the above equation. In addition, the partial pressure of oxygen in the reference electrode, Fe • FeO is fixed by the equilibrium oxygen pressure of the following reaction.

$$Fe + \tfrac{1}{2}O_2 = FeO \tag{39}$$

$$\Delta F_T^o = -RT \ln \frac{1}{P_{O_2}^{\frac{1}{2}}} \tag{40}$$

To obtain the calibration curve of EMF vs. gas composition, the ratio of the flow rates of carbon monoxide and dioxide, and argon and oxygen have been changed to control the oxygen pressure in the gas phase. This method can be applied for any gases in metallurgical works, which are inert against platinum and zirconia electrolyte, such as H_2-H_2O mixtures, SO_2-SO_3 mixtures, top gas of the blast furnace, etc.

Preparation of the Cells and Experimental Procedure

Three types of oxygen concentration cells with the reference electrode of Fe • FeO, Ni - NiO, and Cu • Cu_2O have been constructed. The schematic diagram of the cell is shown in Figure 16 and Photograph 2. The commercial stabilized zirconia tubes, which are supposed to be gas tight up to 10^{-6} mm Hg and up to 1000°C, have been used as the solid electrolyte.

A mixture of pure iron powder and wüstite powder was stamped into the bottom of the zirconia tube along with platinum lead wire. The electrolyte tube was 2 feet long, 3/4 inch outside diameter and 5/8 inch inside diameter.

Platinum wire of 0.005 inch diameter was wound on the outside of the bottom end of the tube and connected to the 0.020 inch platinum lead wire. Wustite slurry was sometimes put on this platinum winding as the solvent for oxygen.

In the cell with the Ni - NiO reference electrode, only the platinum winding was used without the wüstite.

After construction of the cell, it was set into the reaction chamber at room temperature and purified argon gas was injected into the

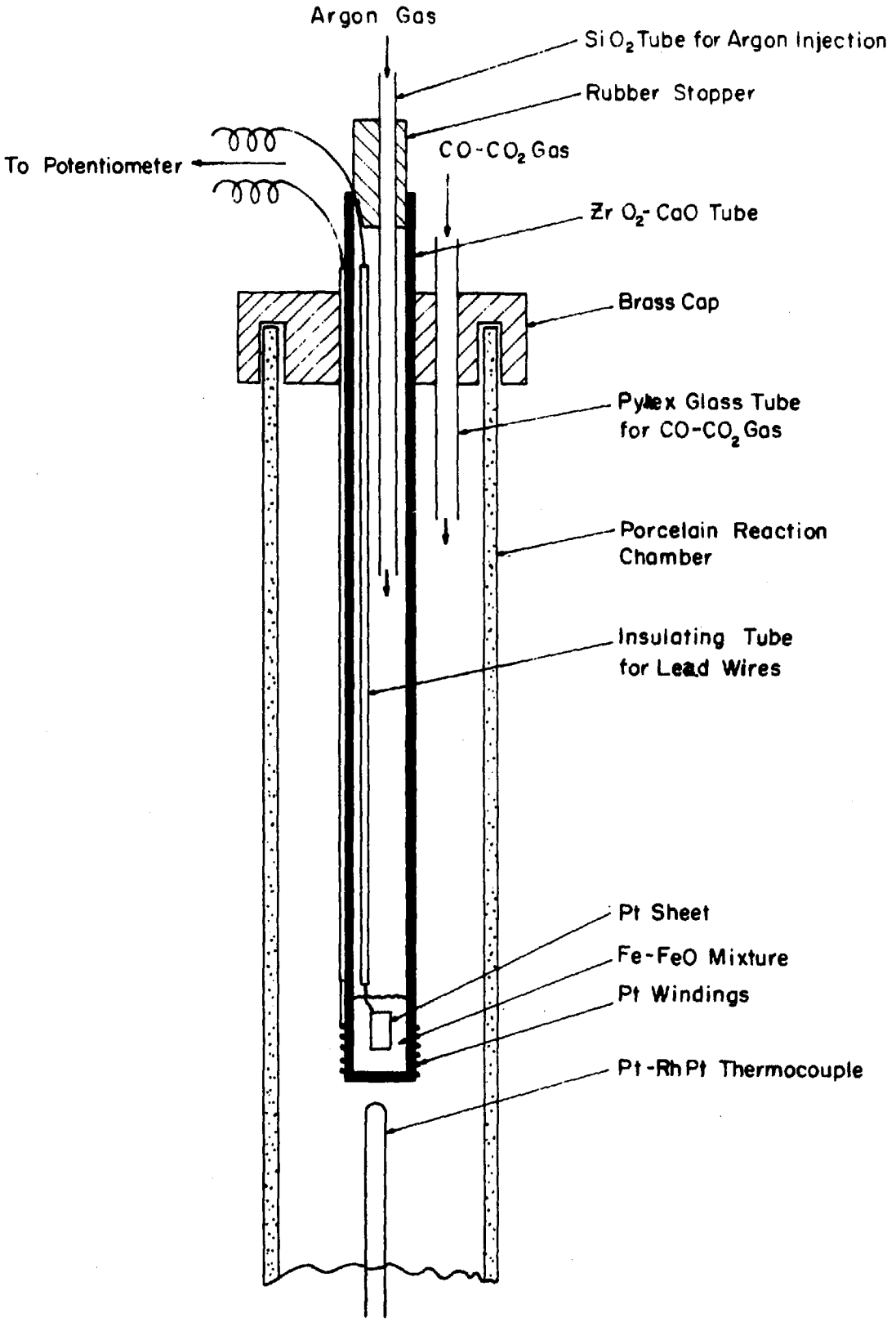

Fig. 16. Schematic Diagram of the Oxygen Gauge.

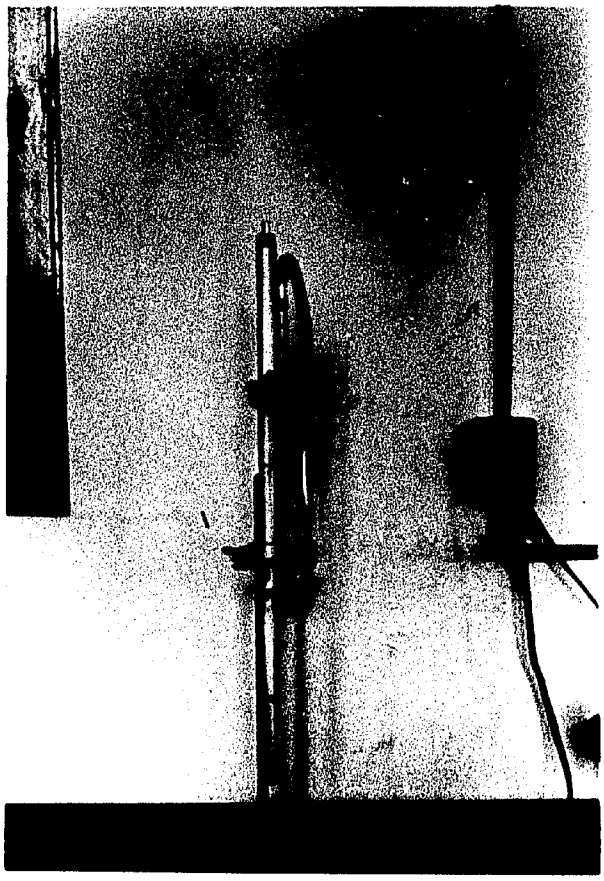

Photograph 2. Oxygen Gauge with Ni-NiO Reference Electrode.

cell and CO - CO_2 or Ar - O_2 gas into the reaction chamber. After heating to the experimental temperatures and controlling the flow rates of carbon monoxide and dioxide or argon and oxygen, the electromotive forces were measured by a potentiometer with an external galvanometer several times after stabilization of the EMF, as well as the gas composition and the temperature.

The EMF seemed to respond spontaneously against a change of gas composition but it took about 10 to 20 minutes to have a fixed gas composition by the present gas trains for carbon monoxide and dioxide, depending upon their flow rates. Therefore, the EMF stabilized after 10 to 20 minutes when the flow rate was changed. The EMF responded spontaneously against a temperature change.

Results of Experiments

The results of the electromotive force measurements for the cells are given below and in Tables 7, 8, 9, 10, and 11, respectively.

1. $\begin{matrix}CO\\CO_2\end{matrix}\vdots$ FeO · Pt | ZrO_2 - CaO | Fe · FeO | Pt
   (EMF)

2. $\begin{matrix}CO\\CO_2\end{matrix}\vdots$ Pt | ZrO_2 - CaO | Fe · FeO | Pt
   (EMF)

3. $\begin{matrix}CO\\CO_2\end{matrix}\vdots$ FeO · Pt | ZrO_2 - CaO | Cu · Cu_2O | Pt
   (EMF)

4. $\begin{matrix}\text{Air or}\\\text{Ar} + O_2\end{matrix}\vdots$ Pt | ZrO_2 - CaO | Ni · NiO | Pt
   (EMF)

TABLE 7. ELECTROMOTIVE FORCE MEASUREMENTS OF CO-CO_2 MIXTURES AGAINST AN Fe • FeO REFERENCE ELECTRODE

Data No.	Temperature °C	EMF mV*	CO Flow Rate cm^3(STP)/min	CO_2 cm^3(STP)/min	% CO_2
FF-1	1000	31.85	41.87	27.0	39.20
FF-2	1000	55.95	41.87	42.3	50.26
FF-3	1000	75.54	41.87	61.6	59.53
FF-4	1000	92.48	41.87	82.3	66.52
FF-5	1000	104.86	41.87	108.2	72.10
FF-6	1000	116.65	41.87	127.5	75.28
FF-7	1000	30.56	41.87	27.5	39.64
FF-8	1000	55.25	41.87	44.5	51.52
FF-9	1100	31.16**	41.87	22.3	34.75
FF-10	1100	41.75	41.87	27.0	39.20
FF-11	1100	59.05	41.87	37.2	47.05
FF-12	1100	75.32	41.87	48.9	53.87
FF-13	1100	85.82	41.87	58.3	58.20
FF-14	1100	94.03	41.87	67.2	61.61
FF-15	1100	101.75	41.87	76.4	64.60
FF-16	1100	112.75	41.87	92.4	68.82
FF-17	1100	130.25	41.87	126.1	75.07
FF-18	1200	41.17	41.87	22.3	34.75
FF-19	1200	59.14	41.87	31.3	42.78
FF-20	1200	82.72	41.87	46.7	52.73
FF-21	1200	97.64	41.87	58.9	58.48
FF-22	1200	113.53	41.87	75.9	64.48
FF-23	1200	123.84	41.87	89.9	68.22
FF-24	1200	143.30	41.87	127.5	75.28
FF-25	1300	59.74	41.87	24.5	36.91
FF-26	1300	140.87	41.87	108.9	72.23
FF-27	1300	161.17	41.87	127.5	75.28

*All EMF values in Tables 7, 8, 9, 10 and 11 are the average of the four or five readings.

**This EMF was obtained by keeping the constant temperature and the gas composition for 11 hours.

TABLE 8. ELECTROMOTIVE FORCE MEASUREMENT OF CO-CO_2 MIXTURES AGAINST AN Ni - NiO REFERENCE ELECTRODE

Data No.	Temp. ^oC	Time min.	EMF mV	CO Flow Rate cm^3(STP)/min	CO_2 cm^3(STP)/min	% CO_2
NP-5	1000	30	279.56	41.87	11.3	21.25
NP-6	1000	20	250.83	41.87	25.8	38.15
NP-7	1000	80	227.18	41.87	41.7	49.90
NP-8	1000	20	214.80	41.87	53.7	56.19
NP-9	1000	20	199.43	41.87	72.8	63.49
NP-10	1000	15	188.70	41.87	88.2	67.81
NP-11	1000	15	180.01	41.87	104.2	71.39
NP-12	1000	15	167.02	41.87	131.3	75.82

TABLE 9. ELECTROMOTIVE FORCE MEASUREMENTS OF CO-CO_2 MIXTURES AGAINST A Cu • Cu_2O REFERENCE ELECTRODE

Data No.	Temp. ^oC	Time min.	EMF mV	CO Flow Rate cm^3(STP)/min	CO_2 cm^3(STP)/min	% CO_2
FC-1	800	15	477.87	41.87	81.4	66.03
FC-2	800	20	465.65	41.87	105.4	71.57
FC-3	800	10	458.47	41.87	125.3	74.95
FC-4	800	10	453.49	41.87	140.9	77.09
FC-5	900	15	438.74	41.87	140.9	77.09
FC-6	900	110	449.86	41.87	113.7	73.09
FC-7	900	20	460.35	41.87	90.8	68.44
FC-8	900	25	470.59	41.87	75.7	64.39
FC-9	900	25	483.69	41.87	58.3	58.20
FC-10	900	20	498.09	41.87	44.5	51.52
FC-11	900	28	531.87	41.87	22.2	34.65
FC-12	900	40	562.44	41.87	10.2	19.59
FC-13	900	7 hrs. 45 min.	573.53	41.87	10.2	19.59
FC-16	1000	35	497.11	41.87	39.0	48.23
FC-17	1000	20	478.72	41.87	54.2	56.42
FC-18	1000	20	462.15	41.87	74.3	63.96
FC-19	1000	15	451.44	41.87	89.6	68.15
FC-20	1000	15	440.28	41.87	110.4	72.50
FC-21	1000	15	427.52	41.87	140.9	77.09

TABLE 10. ELECTROMOTIVE FORCE MEASUREMENTS OF AIR AND PURE OXYGEN MIXTURES AGAINST AN Ni • NiO REFERENCE ELECTRODE

Data No.	Time min.	Temperature °C	EMF mV	Direction of Approaching Equilibrium
PN-1	15	800	688.39	downward
PN-2	5	900	639.25	downward
PN-3	3	1200	506.03	downward
PN-4	5	1300	464.04	downward
PN-5	2	1300	464.04	upward
PN-6	2	1200	506.07	upward
PN-7	2	1100	547.16	upward
PN-8	2	1000	590.84	upward
PN-9	2	900	636.27	upward
PN-10	2	800	687.35	upward
PN-11	2	700	729.45	upward
PN-12	2	700	731.56	upward
PN-13	1	800	668.84	downward
		Against O_2 (Pure)		
PN-28	10	900	683.02	--
PN-29	13 hrs. 40 min.	900	682.55	--
PN-14	1	1000	636.81	downward
PN-15	3	1100	595.40	downward
PN-16	1	1200	552.33	downward
PN-20	5	1300	513.31	downward

TABLE 11. ELECTROMOTIVE FORCE MEASUREMENTS OF Ar-O_2 MIXTURES AGAINST AN Ni • NiO REFERENCE ELECTRODE

Data No.	Flow Rate of O_2 cc/min.	Flow Rate of A cc/min.	% O_2	EMF mV
PN-28	119.7	0	100.00	683.02
PN-29	119.7	0	100.00	682.55
PN-30	119.7	33.7	78.03	676.78
PN-31	80.0	33.7	70.36	674.19
PN-32	63.9	33.7	65.47	672.12
PN-33	49.3	33.7	59.40	669.05
PN-34	32.7	33.7	49.25	663.34
PN-35	20.6	33.7	37.94	658.56
PN-36	12.3	33.7	26.74	645.10

The calibration curves of the EMF against gas composition are given in Figures 17, 18, 19, 20, and 21. Some points in Figure 18 were obtained by keeping a constant temperature and gas composition for one night as shown in Table 7; thereby showing that the EMF was very stable for a long time. The calculated values in the figures are given by a chain line based upon the standard free energy[1] of the formation of the oxides.

Discussion of the Results

Comparing the present results with the calculated values of EMF, also shown as in Figures 22 and 23, there are a few percentage differences between them, possibly due to the electronic conduction. However, this difference is not significant so long as reproducible and self-consistent calibration curves are obtained.

Lifetime of the cells was so good that the EMF was constant for several days at a constant gas composition and temperature. However, wustite had a tendency to diffuse rather rapidly through and on the electrolyte, so that the lifetime of the cells with wustite was shorter.

The purpose of the wüstite on the platinum winding was to dissolve the oxygen according to the oxygen pressure as a solvent for oxygen and possibly as a catalyst. However, the response time of EMF against gas composition was immeasurably short, so that this use of wüstite is not necessary. As to industrial application, there might be many applications of this oxygen gauge in metallurgical furnaces. However, the following advantages and disadvantages can be expected.

1. As far as the construction of the cells is concerned, it is rather easy to obtain the necessary materials written above.

2. The calibration should be done by some gases, the oxygen pressure of which has been well established, such as $CO-CO_2$ mixture or H_2-H_2O mixture.

3. The lifetime of the cell may be long but the first cell used above could serve for about 60 hours. However, the lifetime of the cell with Ni-NiO without wüstite on platinum winding may be much longer due to no contamination of the electrolyte (several days).

4. Temperature of the measurement should be above 800° to insure a rapid response and a high transference number for oxygen.

5. The oxygen diffuses through the electrolyte, although it is apparently very slow. Thus, either the metal or the metal oxide in the reference electrode may disappear eventually due to oxidation or reduction.

6. If the output EMF is connected to the automatic recorder, the continuous measurement of the gas composition may be possible.

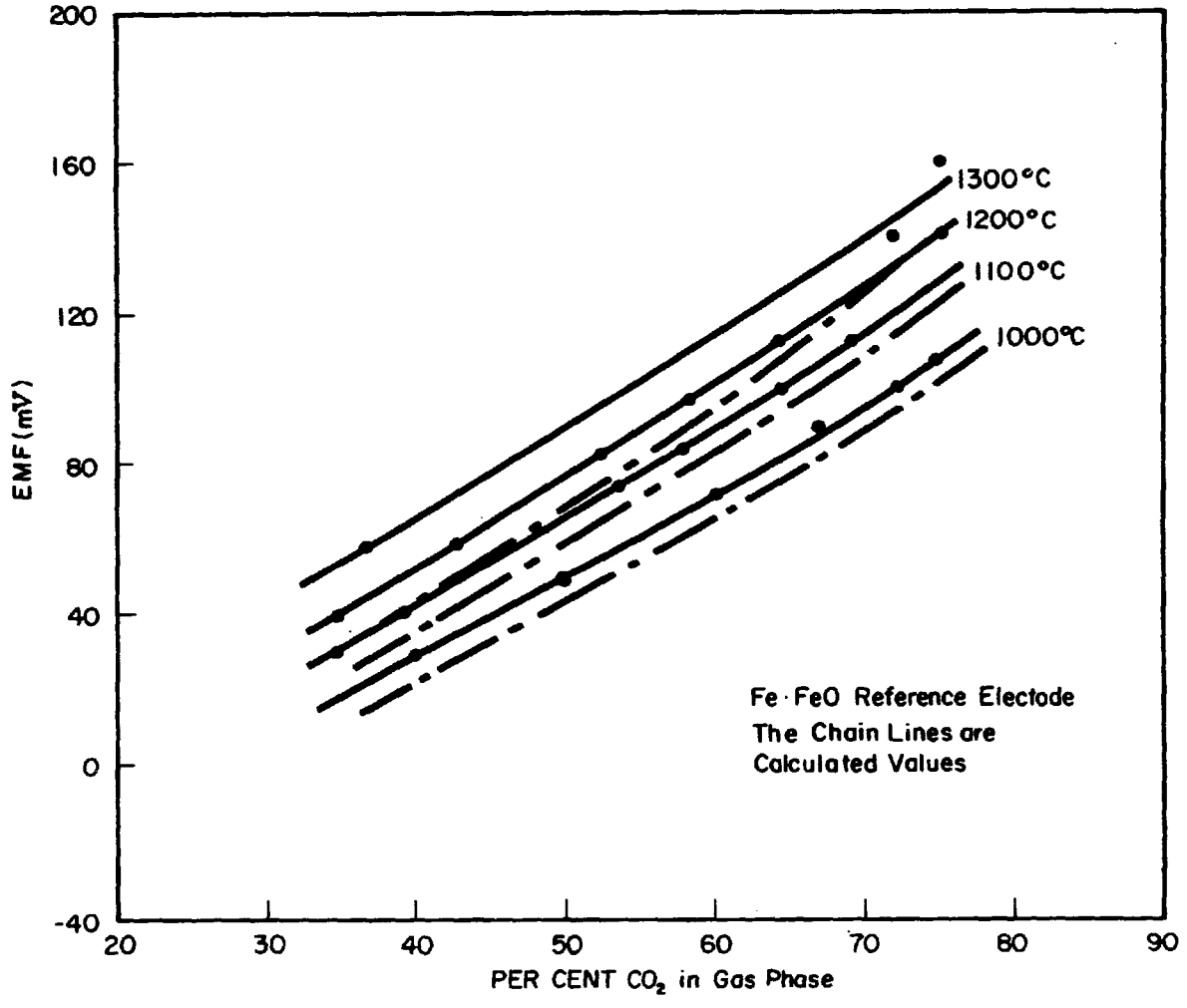

Fig. 17. Calibration Curve of EMF Against $\%CO_2$ in Gas Phase Using Fe • FeO Reference Electrode.

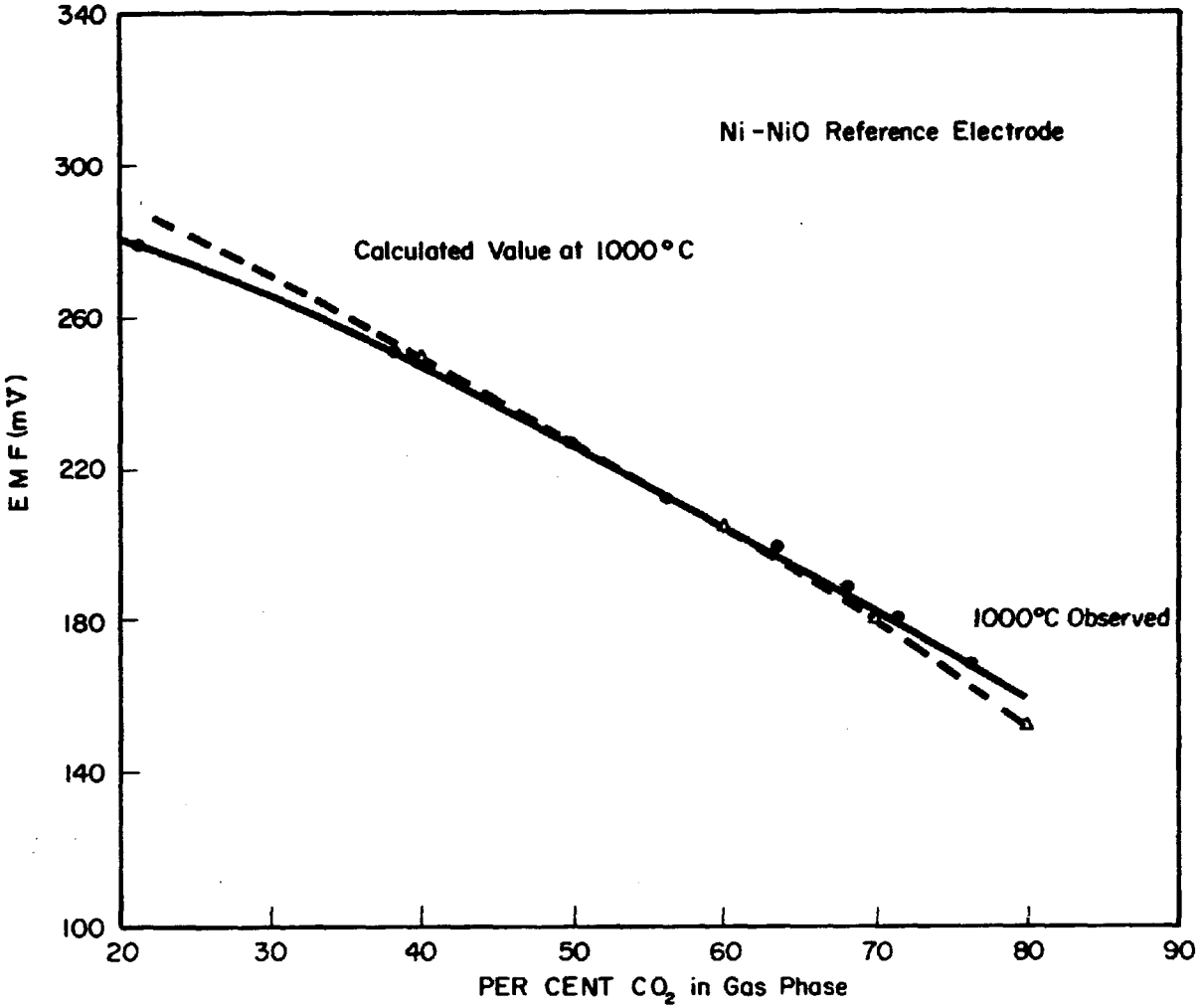

Fig. 18. Calibration Curve of EMF Against $\%CO_2$ in Gas Phase Using Ni - NiO Reference Electrode.

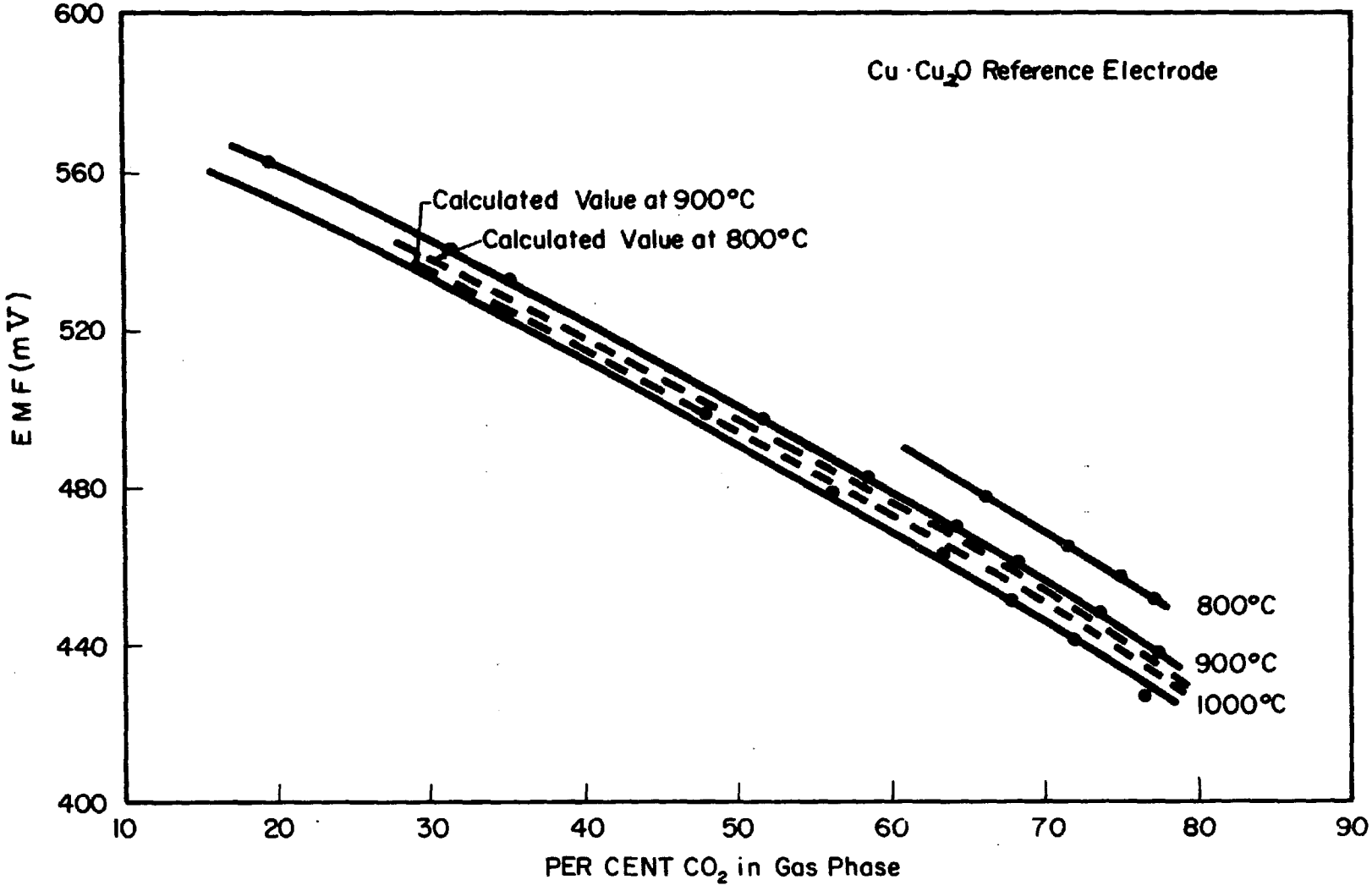

Fig. 19. Calibration Curve of EMF Against $\%CO_2$ in Gas Phase Using Cu • Cu_2O Reference Electrode.

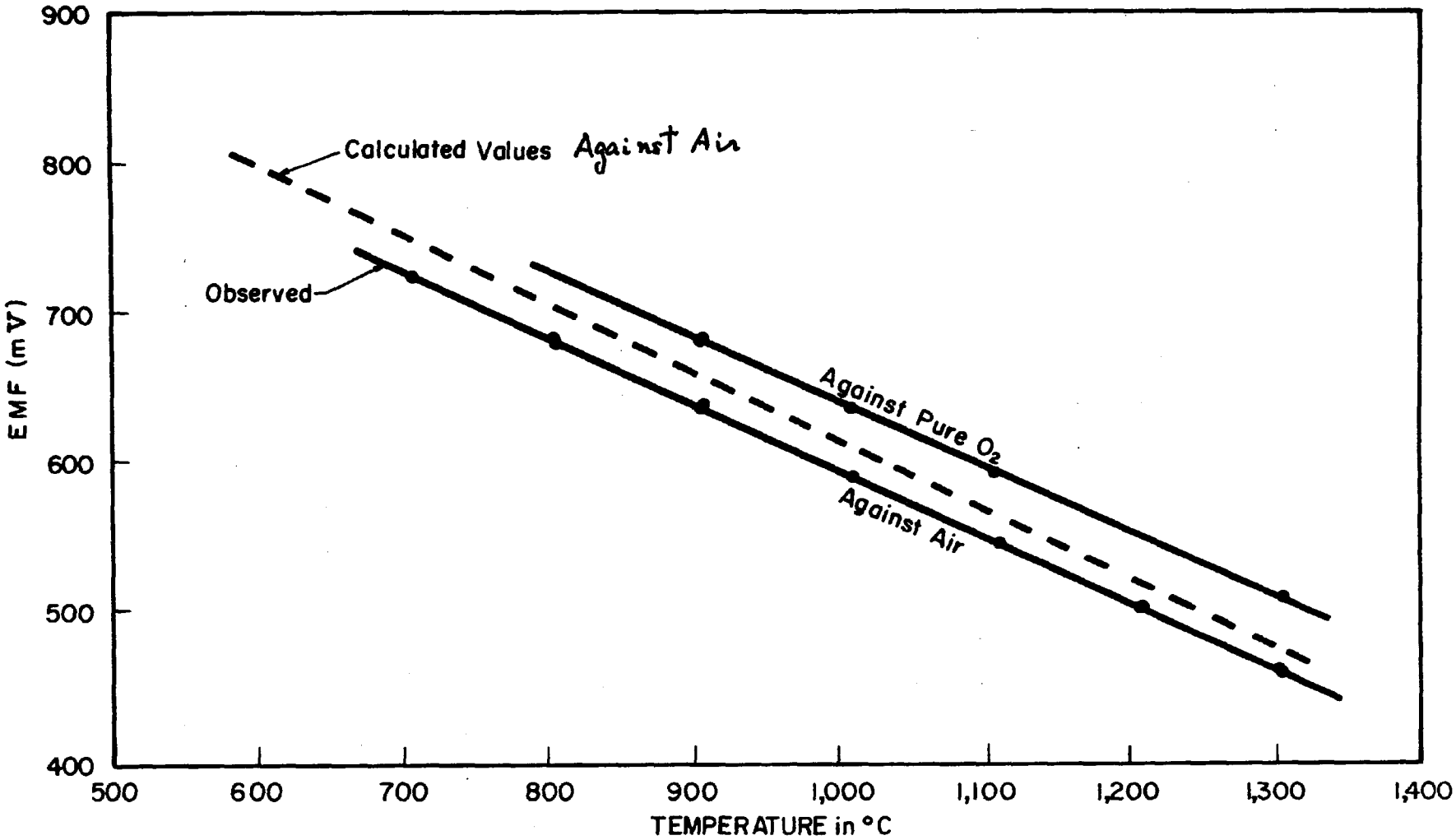

Fig. 20. EMF Against Temperature for Air and Pure Oxygen Measurements.

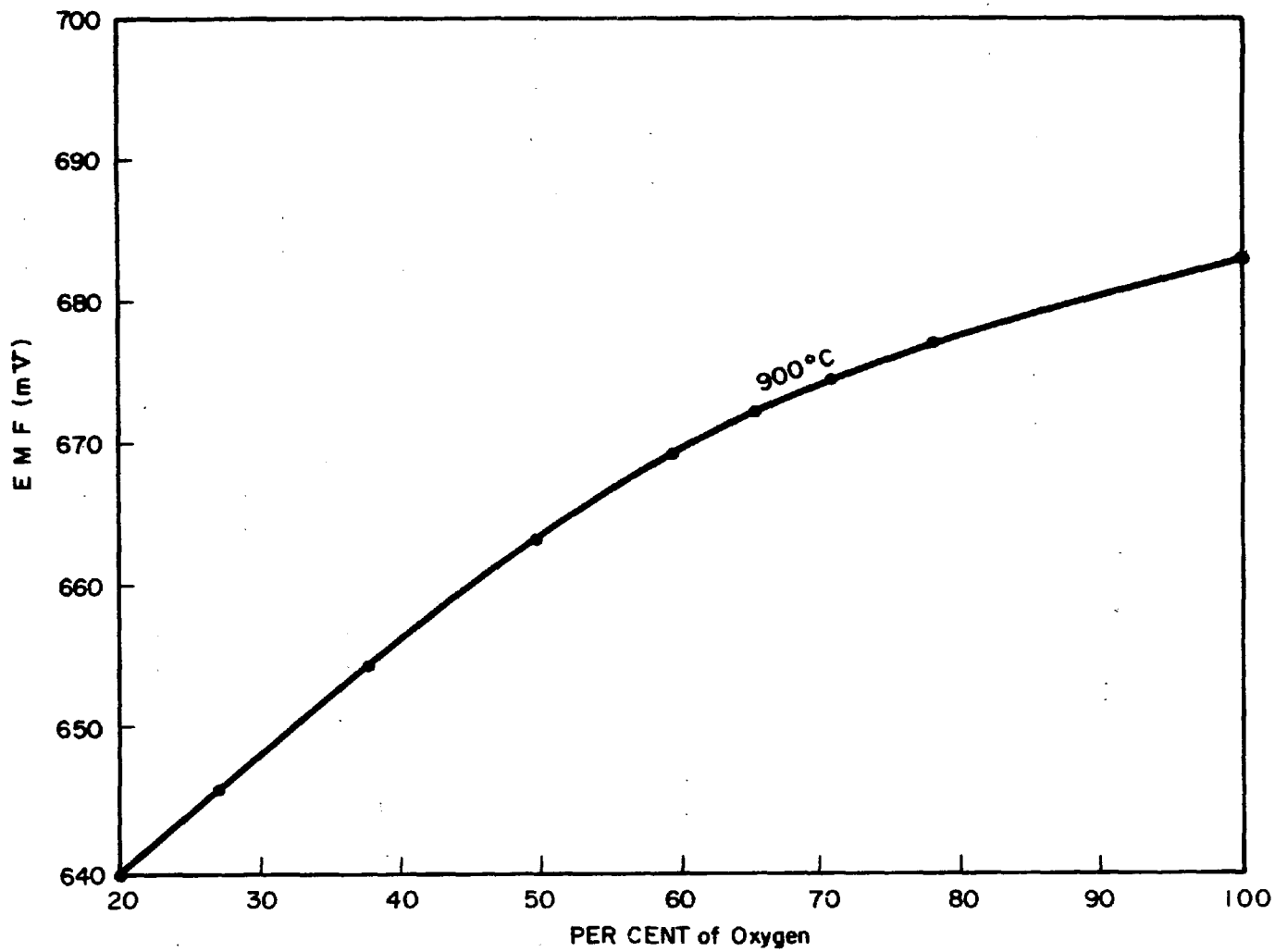

Fig. 21. Calibration Curve of EMF Against % Oxygen in Argon-Oxygen Gas Mixtures.

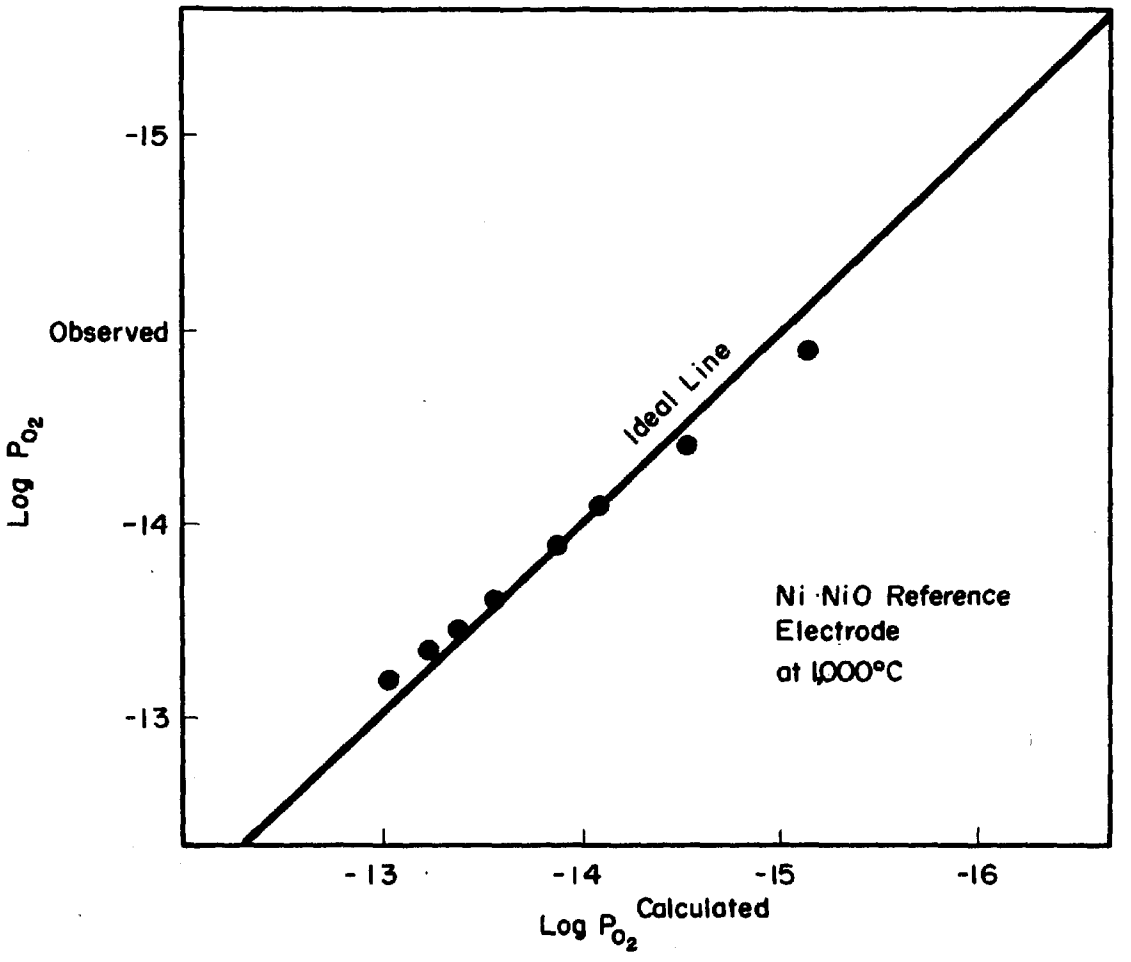

Fig. 22. Relationship between the Observed and Calculated Oxygen Pressures at 1000°C.

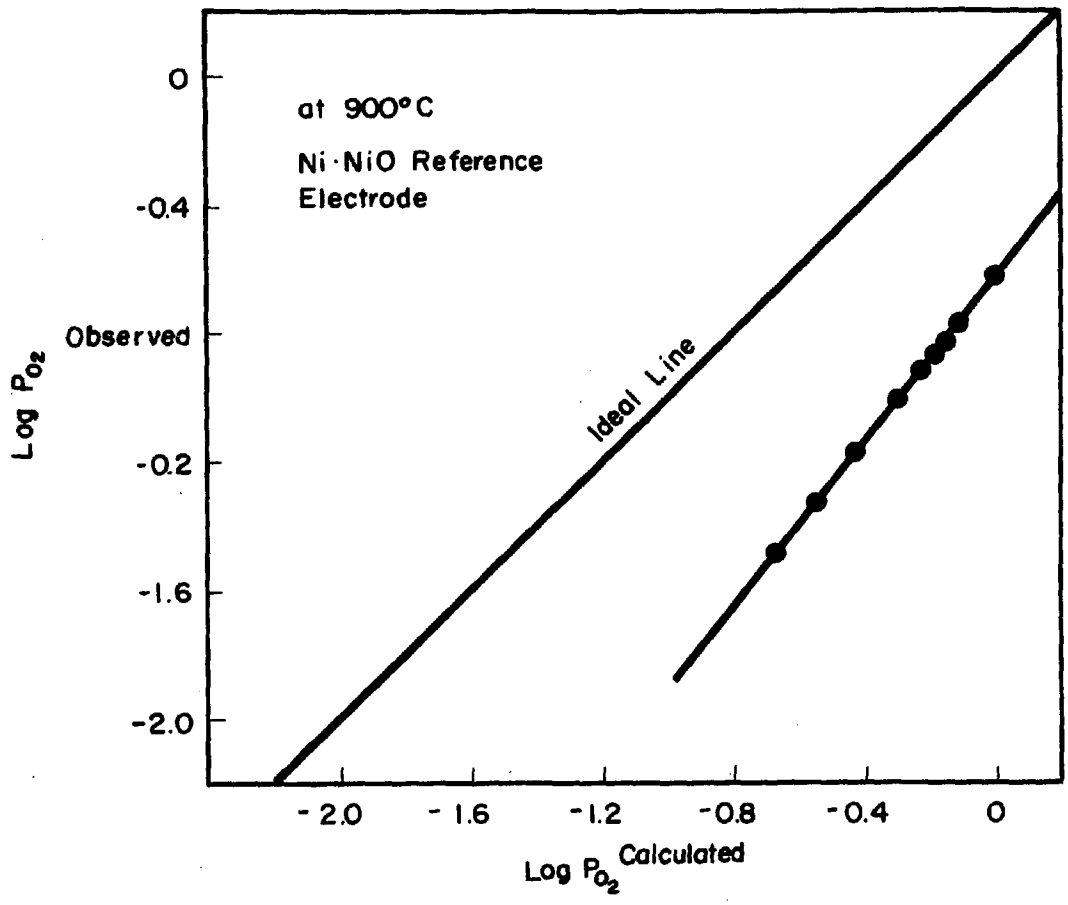

Fig. 23. Relationship between the Observed and Calculated Oxygen Pressures at 900°C.

CHAPTER IV

CONCLUSIONS AND RECOMMENDATIONS FOR FUTURE RESEARCH

Conclusions

By the application of the oxygen concentration cell technique with a solid electrolyte, three kinds of research work have been carried out. The first work was to study the performance of commercial stabilized zirconia as an anion conductor. The standard free energies for the following reactions were obtained.

$$NiO + 2Cu = Cu_2O + Ni \quad (16)$$

$$\Delta F^\circ = 1,570 - 2.87T \ (700^\circ \text{ to } 1050^\circ C) \quad (17)$$

$$FeO + Ni = NiO + Fe \quad (18)$$

$$\Delta F^\circ = 5,280 + 5.88T \ (700^\circ \text{ to } 1200^\circ C) \quad (19)$$

$$\tfrac{1}{2}SnO_2 + Pb = PbO + \tfrac{1}{2}Sn \quad (20)$$

$$\Delta F^\circ = 15,550 - 0.150T \ (600^\circ \text{ to } 850^\circ C) \quad (21)$$

In the second work, the activity of tin in molten lead-tin alloys was determined at 700°, 800°, and 900°C. The activities of tin and lead exhibited positive deviation from ideality and the degree of deviation is smaller at the higher temperature. The free energy of the solution as well as the excess free energy of solution was calculated from activity data. Also the molal quantities of lead and tin in solution were calculated.

In the third experiment, the oxygen gauge was developed and the characteristics of the oxygen gauge as well as calibration data were

obtained. The self-consistent and reproducible EMF against oxygen pressure were successfully obtained by several reference electrodes for oxygen pressure in the range of 10^{-1} to 10^{-20} atm. Also, the lifetime of the oxygen gauge was determined and proved to be long enough for industrial purposes.

Recommendations for Future Research

In the present study, it was demonstrated that the stabilized zirconia could be used as a solid electrolyte with pure anion conduction at high temperature. Thus, this technique can be used to determine the standard free energies of formation of many metallic oxides, which were not yet measured accurately.

Also, the oxygen concentration cell method can be applied to the activity measurement of many metal systems. More improvement on the construction of the cell assembly is also desirable. Finally, the oxygen gauge developed here is desired to be used in industrial furnaces and its performances will be studied in many industrial furnaces.

REFERENCES

1. Elliot, J. F. and Gleiser, M., Thermochemistry for Steelmaking. Addison-Wesley Publishing Co. (1960).

2. Kubaschewski, O. and Catterall, J. A., Thermochemical Data of Alloys. Pergamon Press (1956).

3. Coughlin, J. P., U. S. Bur. Mines Bull. No. 542.

4. Foster, J., "The Tantalum Oxygen System," Master's thesis, Ohio State University (1962).

5. Hund, F., "Die Fluoritphase in System ZrO_2 - CaO," Z. Phys. Chem., 199, 142 (1952).

6. Kiukkola, K. and Wagner, C., "Measurements on Galvanic Cells Involving Solid Electrolyte," J. Electrochem. Soc., 104, 379 (1957).

7. Rapp, R. A. and Maak, F., "The Determination of Activities in Solid Copper-Nickel Alloys Using Galvanic Cells Involving a Solid Electrolyte." Not published.

8. Humphrey, G. L., King, E. G., and Kellog, K. K., Bur. Mines Rpt. Investigations 4870 (1952).

9. Darken, L. S. and Gurry, R. W., "The System Iron-Oxygen," J. Am. Chem. Soc., 67, 1398 (1945).

10. Dingmann, Th., Kirscht, P. H., and Wesselkock, H., Z. anorg. allgem. Chem., 182, 1558 (1956).

11. Gokcen, N. A., J. Metals, 8, 1558 (1956).

12. Coughlin, J. P., King, E. G., and Bonnickson, K. R., "High Temperature Heat Content of Ferrous Oxides, Magnetite and Ferric Oxide," J. Am. Chem. Soc., 73, 3891 (1951).

13. Treadwell, W. D., "Uber Den Sauerstoffdnick Einiger Oxyde Und Die Kohl-Sauerstoffkette bei Höherer Temperatur," Z. Elektrochem., 22, 414 (1916).

14. Schenk, R. and Wesselkock, H., Z. anorg. allgem. Chem., 184, 39 (1929).

15. Watanabe, M., Sci. Repts. Imp. Tohoku University, I, 22, 436 (1933).

16. Fricke, R. and Weitbrecht, G., "Die Gleichgewichte CO_2/CO Gegen Ni/NiO, BZW. Ni + - $Al_2O_3/NiAl_2O_4$ und Ihre Beeinflüssung Durch Den Physikalishen Zustund der Festen Reactionsteilnehmer," Z. Elecktrochem., 48, 87 (1942).

17. Kleppa, O. J., "A New High-Temperature Reaction Calorimeter," J. Phys. Chem., 59, 175, 354 (1955).

18. Elliott, J. F. and Chipman, J., "The Thermodynamic Properties of Liquid Ternary Cadmium Solutions," J. Am. Chem. Soc., 73, 2682 (1951).

19. Alcock, C. B., Physical Chemistry and Technology of the Steelmaking Conference to Commemorate the Career of John Chipman. Massachusetts Institute of Technology, June, 1962.

20. Weissbart, J. and Ruka, R., "Oxygen Gauge," Scientific Instruments, 593, 32 (1961).

21. Schmalzried, H., "Concerning Zirconia as an Electrolyte for Electrochemical Investigation at High Temperature," Private communication.

22. Kingery, W. D., Pappis, J., Doty, M. E., and Hill, D. C., "Osygen Ion Mobility in Cubic $Zr_{0.85}$ $Ca_{0.15}$ $O_{1.85}$," J. Am. Chem. Soc., 393, 42 (1959).

AUTOBIOGRAPHY

I, Kazuhiro Goto, was born in Sendai, Japan, January 18, 1936. I received my high school education in Sendai First High School, Sendai, Japan, and my undergraduate training at Tohoku University, Sendai, Japan, which granted me the Bachelor of Engineering degree in 1958. From Tohoku University, I received the Master of Engineering degree in 1960. In September, 1960, I was appointed University Research Fellow at Ohio State University, where I specialized in the Department of Metallurgical Engineering. I held this position for two years while completing the requirements for the Doctor of Philosophy degree.

I have accepted a position as research assistant in Metallurgy at Tokyo University.